in the process of hepatocarcinogenesis in LEC rats. We also examined protein expression of these G1 phase-related cell cycle molecules. Furthermore, we evaluated not only total amounts of pRb but also amounts of phosphorylated pRb in hepatocarcinogenesis.

Materials and methods

Animals. LEC rats were maintained under specific pathogen-free conditions in the Institute for Animal Experimentation, University of Tokushima School of Medicine and coded as Tj (Tokushima, Japan). Animals were sacrificed when they were 2-, 6- or 18-month-old. Each group consisted of 6 animals.

Histological analysis. For routine histological analysis, rats were anesthetized by diethyl ether and the abdomen was opened. The liver was then perfused from the portal vein with 50 ml of phosphate-buffered saline to clear it of blood and fixed in 10% neutral-buffered formalin. After fixation, the livers were embedded in paraffin for hematoxylin-eosin staining.

RNA extraction and reverse transcription. Chemicals were purchased from Sigma Chemical Co. (St. Louis, MO, USA) or Wako Pure Chemical Co. (Tokyo, Japan), unless otherwise mentioned. Total RNA was isolated from approximately 30 mg of liver tissues, using the RNeasy Protect Mini Kit (Qiagen, Hilden, Germany) according to the manufacturer's instructions. Complementary DNA (cDNA) was synthesized in a 30 μl reaction volume. A sample of total RNA (2 μg) was incubated at 65°C for 10 min, and then cooled for 2 min on ice. A sample was transferred to the tube of the Ready-To-Go You-Prime First-Strand Beads (Amersham Biosciences, Piscataway, NJ, USA) and incubated for 1 min at room temperature with the oligo-dT primers (Invitrogen, Carlsbad, CA, USA). The reaction was then incubated at 37°C for 60 min. The obtained cDNA was used for quantitative real-time polymerase chain reaction (PCR).

Quantitative real-time PCR. Quantitative PCR was performed by the real-time PCR system, LightCycler (Roche Diagnostics, Mannheim, Germany), using the SYBR Green I double strand DNA binding dye (Roche Diagnostics). The amplification of a target with the primers listed in Table I was carried out in a total volume of 20 μl containing 0.3 μM of each primer, 3 mM $MgCl_2$, 2 μl of master mixture (LightCycler FastStrand DNA Master SYBR Green I) and 1 μl of template cDNA. The reaction mixture was preheated at 95°C for 10 min, followed by 40 cycles at 95°C for 10 sec, 62°C for 10 sec and 72°C for 7 sec. Fluorescence data were collected after each extension step. Melting curve analysis was performed by heating the PCR product at 95°C, then cooling to 65°C and finally raising to 95°C with a 0.1°C/second temperature transition rate while continuously monitoring the fluorescence. Fluorescence was analyzed by using the LightCycler Software version 3.5 (Roche Diagnostics). The crossing point for each reaction was determined and manual baseline adjustment was made. To quantify and prove the integrity of isolated RNA, real-time PCR analysis for glyceraldehyde-3-phosphate dehydrogenase (GAPDH) was also carried out. Each run consisted of GAPDH as an internal standard and a negative control without samples.

Table I. Primers used for real-time RT-PCR.

Gene	Primers
GAPDH	Forward: 5'-TGAACGGGAAGCTCACTGG-3'
	Reverse: 5'-TCCACCACCCTGTTGCTGTA-3'
Cyclin D1	Forward: 5'-GGGAAGTTTTGTTCTCTTTG-3'
	Reverse: 5'-TAGTTGATTACTGGGGTACA-3'
Cdk4	Forward: 5'-TGTATCTTCGCAGAGATGTT-3'
	Reverse: 5'-GATTAAAGGTCAGCATTTCC-3'
Cdk6	Forward: 5'-GACCTTTGAGCACCCCAACG-3'
	Reverse: 5'-TCCAGACCTCGGAGAAGCTGA-3'

Antibodies. All primary and secondary antibodies were purchased from Santa Cruz Biotechnology (Santa Cruz, CA, USA). Optimal dilutions of antibodies used for Western blotting in this study were as follows: monoclonal antibody A-12 (anti-cyclin D1), 1:100; polyclonal antibody C-22 (anti-Cdk4), 1:100; polyclonal antibody C-21 (anti-Cdk6), 1:100; polyclonal antibody C-15 (anti-pRb), 1:200; polyclonal antibody Ser 780 (anti-phosphoserine pRb), 1:100; horseradish peroxidase anti-mouse immunoglobulin G (IgG), 1:1000; horseradish peroxidase anti-rabbit IgG, 1:1000. Antibody C-15 against pRb recognizes both phosphorylated and non-phosphorylated pRb. Conversely, the phosphoserine pRb polyclonal antibody (Ser 780) reacts only with phosphorylated pRb at Ser 780. Cyclin D1/Cdk4 complex specifically phosphorylates Ser 780 in pRb.

Tissue lysates. The tissue samples were frozen on dry ice within 20 min after collection. The tissue lysates were prepared as described in our previous report (11). Protein concentrations of the lysates were determined using the Bio-Rad (Hercules, CA, USA) protein assay kit with bovine serum albumin as standard.

Gel electrophoresis and Western blotting. For Western blot analysis, protein extracts were added to an equal volume of sample buffer. Sodium dodecyl sulfate-polyacrylamide gel electrophoresis (SDS-PAGE) was performed according to the Laemmli method (12) by loading 50 μg of protein in each lane. After electrotransfer onto a nitrocellulose membrane (Millipore, Billerica, MA, USA) and blocking with a 5% milk solution in Tris buffered saline (TBS) containing 0.1% Tween-20, Western blots were incubated overnight with anti-cyclinD1, anti-Cdk4, anti-Cdk6, anti-pRb or anti-phosphoserine pRb antibodies. As secondary antibodies, horseradish peroxidase anti-rabbit IgG or horseradish peroxidase anti-mouse IgG were used. The antigen-antibody complexes were visualized by using an enhanced chemiluminescence detection system (Amersham) on a radiography film. Exposures were made for 30 sec at room temperature for all samples.

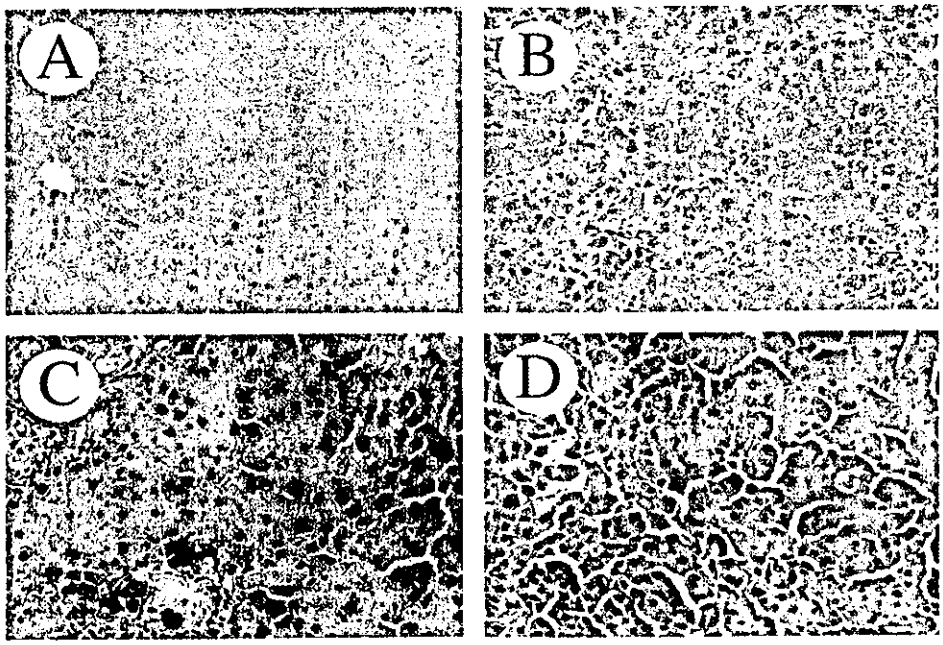

Figure 1. Histological analysis of the liver of LEC rats. Liver tissues obtained from LEC rats at various time points were examined histologically by hematoxylin-eosin staining. The liver of 2-month-old LEC rats demonstrated normal hepatic architecture with normal hepatocytes (A). The liver of 6-month-old LEC rats revealed a chronic hepatitis pattern, such as the disarray of normally radial hepatocyte alignment and mild infiltration of inflammatory cells (B). The liver obtained from 18-month-old LEC rats demonstrated severe dysplasia with nuclear crowding (C) and contained a number of macroscopic nodules that were diagnosed to be well-differentiated HCC (D). Representative pictures are shown in the figure. Original magnification x200.

Densitometric analysis. The densities of the immunoreactive bands of the various G1 phase-related cell cycle proteins obtained by autoradiography were estimated quantitatively by means of densitometric scanning (Tlc scanner; Shimazu Co., Kyoto, Japan).

Statistical analysis. Data are expressed as means ± SEM. The significance of differences between observations was determined by Scheffe's multiple comparison method. A $p<0.05$ was considered to indicate a significant difference between groups.

Results

Histological examination of the liver of LEC rats. Two-month-old LEC rats were sacrificed and liver tissues were obtained. Six-month-old and 18-month-old LEC rats that survived severe acute hepatitis were also sacrificed for collecting liver tissues. Each group consisted of 6 animals. Liver tissues obtained from 2-month-old LEC rats revealed normal hepatic structure with normal hepatocytes (Fig. 1A). Conversely, those obtained from 6-month-old LEC rats revealed rearrangement of basic architecture of liver acinus, disarray of normally radial liver-cell alignment, variation in size of hepatocytes, increase of Kupffer cells and mild infiltration of inflammatory cells, which were characteristic of chronic liver injury in LEC rats (Fig. 1B). Liver tissues obtained from 18-month-old LEC rats revealed the disappearance of hepatic cords and severe dysplasia of hepatocytes with nuclear crowding (Fig. 1C). Although these findings were not malignant, liver tissues of 18-month-old LEC rats were considered to be a precancerous condition. Furthermore, there were a number of macroscopic yellowish nodules in the liver of all the 18-month-old LEC rats. Some nodules were diagnosed histologically as HCC (Fig. 1D) and others were as cholangiofibrosis (data not shown). According to these histological findings, liver tissues of 2- and 6-month-old LEC rats were considered to be normal and chronic hepatitis livers, respectively. Liver tissues without macroscopic nodules of 18-month-old LEC rats were used as precancerous liver. Macroscopic nodules contained in livers of 18-month-old LEC rats and confirmed histologically to be HCC but not cholangiofibrosis were used as HCC tissues for the subsequent experiments.

mRNA expression of G1 phase-related cell cycle molecules in the liver of LEC rats. To examine the role of G1 phase-related cell cycle molecules in the process of hepatocarcinogenesis in LEC rats, we determined mRNA expression levels of cyclin D1, Cdk4 and Cdk6 in the liver of LEC rats, using quantitative real-time PCR. As shown in Fig. 2A, cyclin D1 mRNA expression was increased markedly in chronic hepatitis liver of 6-month-old LEC rats and approximately 8-fold higher compared with that in normal liver of 2-month-old ones. Notably, it was then decreased significantly in pre-cancerous liver and HCC tissues of 18-month-old rats compared with chronic hepatitis livers of 6-month-old ones. However, levels of cyclin D1 mRNA expression in pre-cancerous liver and HCC were significantly higher than those in normal liver.

mRNA expression of Cdk4 and Cdk6 in the liver of LEC rats was then evaluated. Although mRNA levels of Cdk4 did

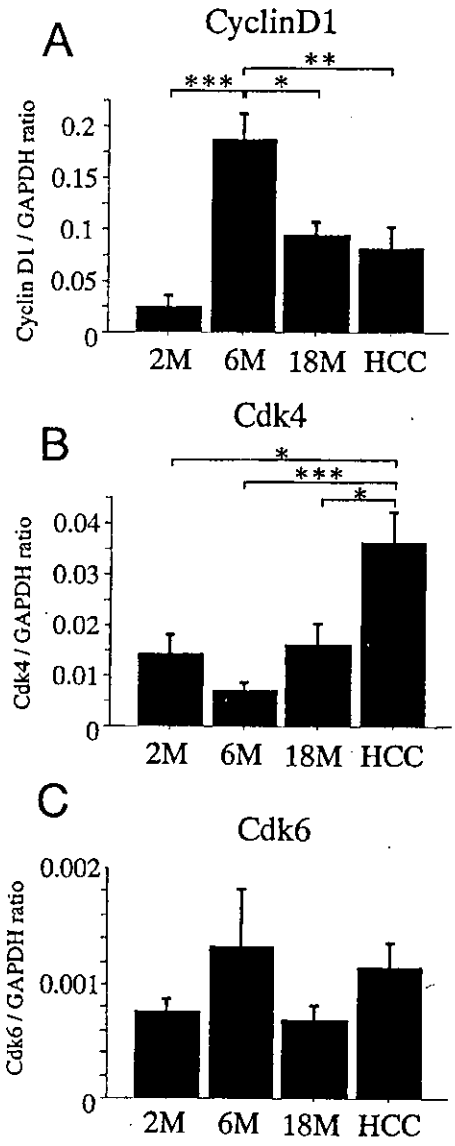

Figure 2. mRNA expression of cyclin D1, Cdk4 and Cdk6 in the liver of LEC rats. To quantitatively estimate mRNA expression of cyclin D1, Cdk4 and Cdk6 in the liver of LEC rats, a real-time PCR method was employed. The value of each amplified message was standardized by the amount of GAPDH quantified from the same sample. Cyclin D1 mRNA expression was increased in chronic hepatitis liver then decreased in precancerous liver and HCC (A). Although Cdk4 mRNA expression was not significantly different among normal, chronic hepatitis and precancerous livers, it was significantly increased in HCC (B). Cdk6 mRNA expression did not show significant changes during hepatocarcinogenesis in LEC rats (C). Values are expressed as means ± SEM of 5 separate experiments. 2M, 6M, 18M and HCC represent the normal liver of 2-month-old LEC rats, chronic hepatitis liver of 6-month-old LEC rats, precancerous liver and HCC of 18-month-old LEC rats, respectively. This definition is also used in Figs. 3 and 4. $^{*}0.01<p<0.05$; $^{**}0.001<p<0.01$; $^{***}p<0.001$.

not change significantly among normal liver of 2-month-old LEC rats, chronic hepatitis liver of 6-month-old ones and precancerous liver of 18-month-old ones, they were increased significantly in HCC of 18-month-old LEC rats (Fig. 2B). Conversely, mRNA levels of Cdk6 did not change significantly among these liver tissues (Fig. 2C), indicating that Cdk6 mRNA expression did not change significantly during hepatocarcinogenesis in LEC rats.

Protein expression of G1 phase-related cell cycle molecules in the liver of LEC rats. To examine protein expression of cyclin D1, Cdk4 and Cdk6, the same protein amount of the lysate samples was mixed in each experimental group and the resulting mixtures containing 30 mg of protein were applied on SDS-PAGE for Western blotting. The upper and lower panels in Fig. 3 show the results of Western blot and densitometric analyses, respectively.

Immunoreactive bands for cyclin D1 were detected at a molecular weight of 36 kDa in the liver tissues of 2-, 6- and 18-month-old LEC rats. The densitometric analysis revealed that cyclin D1 protein expression was low not only in normal liver but also in HCC, while it was increased in chronic hepatitis and precancerous livers, indicating that protein expression of cyclin D1 was increased as the course of chronic hepatitis, and then decreased in HCC.

Immunoreactive bands for Cdk4 were observed at a molecular weight of 34 kDa. Expression levels of Cdk4 protein were increased during the process of hepatocarcinogenesis in LEC rats. The densitometric analysis demonstrated that the amounts of Cdk4 in chronic hepatitis liver, precancerous liver and HCC were 1.7-, 1.9- and 2.4-fold higher, respectively, than those in normal liver of LEC rats. Immunoreactive bands for Cdk6 were detected at a molecular weight of 37 kDa. In contrast to Cdk4, there was no tendency in Cdk6 protein expression during hepatocarcinogenesis in LEC rats.

Levels of pRb and phosphorylated pRb in the liver of LEC rats. Western blot analyses for pRb and phosphorylated pRb in the liver of LEC rats were performed (Fig. 4). pRb is phosphorylated by cyclin D1/Cdk4 and cyclin D1/Cdk6 during G1/S transition. Because this phosphorylation causes the inactivation of the growth inhibitory functions of pRb, phosphorylation of pRb is the ultimate event for the transition from G1 to S phase. Immunoreactive bands for pRb and phosphorylated pRb were observed at molecular weights of 110 kDa, respectively (Fig. 4, upper panels). The densitometric analysis of the immunoreactive bands are shown in Fig. 4, lower panels. The amount of pRb did not change at all among normal, chronic hepatitis and precancerous liver of LEC rats. Furthermore, increased pRb protein expression was not observed even in HCC. In marked contrast, phosphorylated pRb was barely detected in the liver of 2-month-old LEC rats. However, considerable amounts of phosphorylated pRb were detected not only in chronic hepatitis but also in precancerous liver. Amounts of phosphorylated pRb were further increased in HCC compared with normal and precancerous livers.

Discussion

Cell cycle-related molecules play essential roles in carcinogenesis. Specifically, G1 phase-related cell cycle molecules are important, because they are requisite for the entry into the cell cycle from the quiescent state. Cell cycle-related molecules are mainly divided into 3 groups, namely cyclins,

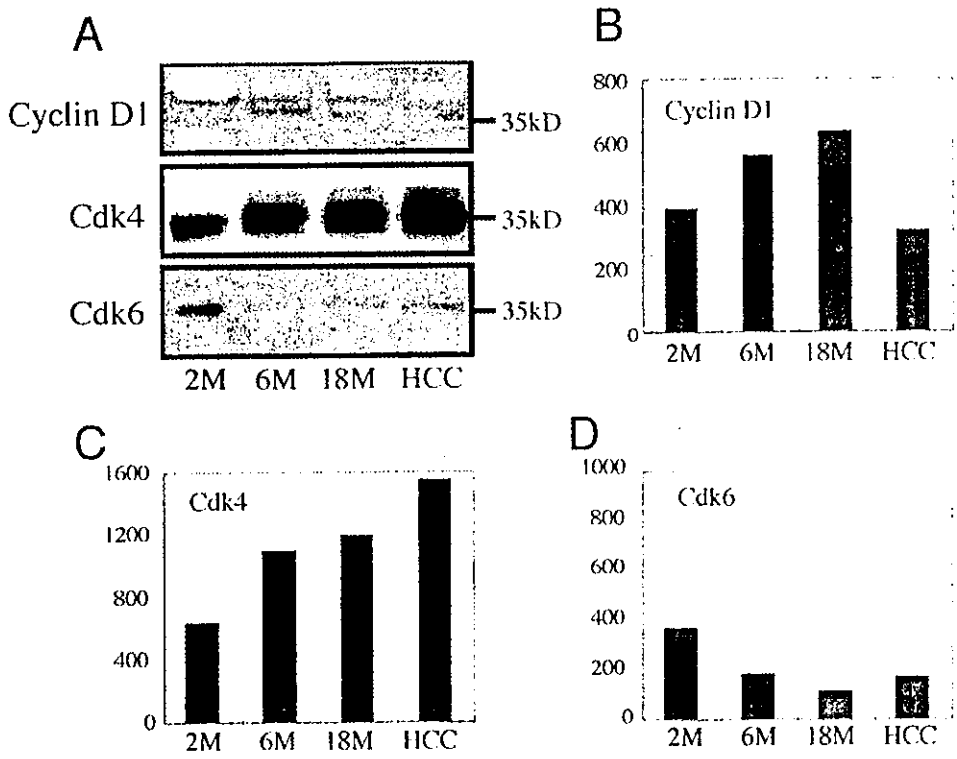

Figure 3. Protein expression of cyclin D1, Cdk4 and Cdk 6 in the liver of LEC rats. To quantitatively evaluate protein expression of cyclin D1, Cdk 4 and Cdk6 in the liver of LEC rats, Western blot (A) and densitometric analysis were performed. Cyclin D1 protein expression was decreased in the course of chronic hepatic inflammation and then decreased in HCC (B). Cdk4 protein expression was increased gradually during hepatocarcinogenesis in LEC rats and the highest in HCC (C). Cdk6 protein expression did not show any tendency during hepatocarcinogenesis in LEC rats (D). The protein level in 2-month-old rat liver was used as the reference level (=1).

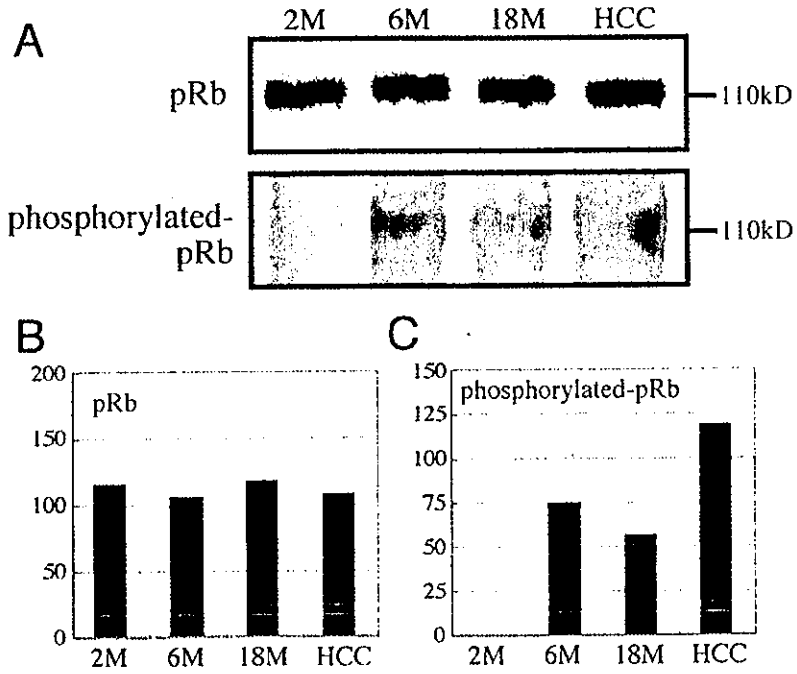

Figure 4. Amounts of pRb and phosphorylated pRb in the liver of LEC rats. To quantitatively evaluate the amounts of pRb and phosphorylated pRb in the liver of LEC rats, Western blot (A) and densitometric analyses were performed. Total amounts of pRb including phosphorylated and non-phosphorylated pRb were not different at all among normal, chronic hepatitis, precancerous livers and HCC (B). In marked contrast, phosphorylated pRb was hardly detectable in normal liver and increased substantially in chronic hepatitis and precancerous liver (C). Levels of phosphorylated pRb were further increased in HCC.

Cdks and Cdk inhibitors. Among cyclins, the D-type (D1, D2 and D3), specifically cyclin D1, serves as a critical regulator of the cell cycle (13). The cyclin D1 gene has been identified as a target gene in the Wnt signaling pathway as well as the Ras-activated mitogen-activated protein kinase signaling pathway. Increased protein expression of cyclin D1 has been demonstrated in various types of cancers including HCC (14-21). It has been shown that increased levels of cyclin D1 were associated with aggressive HCC (22-25) and with poor prognosis in HCC (26). Furthermore, transgenic mice overexpressing the cyclin D1 gene in the liver were shown to develop HCC with the passage of time (27), indicating that overexpression of cyclin D1 may be sufficient to initiate hepatocarcinogenesis. However, in marked contrast, targeted overexpression of the cyclin D1 gene to the oral cavity and esophageal epithelium of transgenic mice led to dysplasia in the esophagus but progression to esophageal carcinoma was not observed (28,29). Thus, it is not clear whether increased cyclin D1 protein is a cause or a consequence of carcinogenesis.

We have shown here that mRNA levels of cyclin D1 were markedly increased in chronic hepatitis liver compared with normal liver. The mRNA levels were then decreased during the chronic inflammatory process of the liver and significantly lower in precancerous liver surrounding HCC. Furthermore, there were no significant differences in cyclin D1 mRNA level between HCC and the surrounding non-cancerous tissues. Similar results were confirmed by the Western blot analysis. Protein levels of cyclin D1 were increased in the liver with the passage of chronic hepatic inflammation and then decreased in HCC. The result of cyclin D1 mRNA expression was different from that of cyclin D1 protein expression in precancerous liver tissues, suggesting the rapid post-transcriptional degradation of cyclin D1 in the precancerous liver. Furthermore, it has been shown that cyclin D1 expression is markedly increased in rodent livers after partial hepatectomy (30-33). It has also been shown that cyclin D1 induction is one of the earlier events in hepatocyte proliferation induced by thyroid hormone, suggesting that cyclin D1 may be a common target responsible for the mitogenic activity of ligands of nuclear receptors (34). Furthermore, it has been shown by differential hybridization of cDNA arrays and RNase protection studies that early stimulated expression of cyclin D1 was induced in the murine liver treated with CCl_4 that causes liver injury but not hepatocarcinogenesis (35). Furthermore, Albrecht *et al* (36) have demonstrated the increased cyclin D1 expression in human liver tissues from various acute and chronic liver diseases, and stated that cyclin D1 may eventually provide a clinically relevant molecular marker of regenerative activity in human liver diseases. We also demonstrated here that cyclin D1 might play a major role in hepatocyte proliferation but not in hepatocarcinogenesis, because its expression was increased in the course of chronic hepatic inflammation and decreased in HCC. Taken collectively, these results indicate that the induction of cyclin D1 plays an essential role in hepatocyte proliferation without hepatocarcinogenesis.

We have shown here that mRNA expression of Cdk4 was significantly higher in HCC than normal, chronic hepatitis and precancerous livers. Protein levels of Cdk4 increased gradually in the process of hepatocarcinogenesis and were the highest in HCC compared with normal, chronic and precancerous livers. In contrast, Cdk6 expression did not show any significant changes during the process of hepatocarcinogenesis either in the mRNA level or in the protein level. These results indicate that Cdk4 but not Cdk6 may play an important role in the process of transition from chronic hepatitis to HCC in LEC rats. Cyclin D1 forms complexes with Cdk4 and also with Cdk6. Therefore, the cyclin D1-related kinase activities can be expressed as the sum of cyclin D1/Cdk4 and cyclin D1/Cdk6 kinase activities. It has been shown that in the regenerating liver of mice after partial hepatectomy, cyclin D1 formed complexes with Cdk4, which were markedly activated in the regenerating liver, but not with Cdk6. We have shown here that mRNA and protein expression of cyclin D1 was markedly elevated in chronic hepatitis liver than in normal liver. We have also shown that mRNA and protein expression of Cdk4 was higher in the chronic hepatitis liver than in the normal liver. Therefore, enhanced kinase activity of cyclin D1/Cdk4 was considered to be responsible for hepatocyte proliferation in chronic hepatitis.

pRb is the ultimate substrate of cyclin D1/Cdk4 and cyclin D1/Cdk6 complexes in the pathway leading to transition from G1 to S phase (37). pRb controls gene expression mediated by a family of heterodimeric transcriptional regulators, collectively termed the E2Fs, which can transactivate genes whose products are essential for S phase entry. In its phosphorylated form, pRb binds to a subset of E2F complexes, converting them to repressors that constrain expression of E2F target genes. Phosphorylation of pRb frees these E2Fs, enabling them to transactivate the same genes, a process initially triggered by cyclin D1/Cdk4 and cyclin D1/Cdk6 complexes, and then accelerated by cyclin E/Cdk2 complexes. In the present study, total amounts of pRb including phosphorylated and non-phosphorylated pRb did not show any significant changes among normal, chronic hepatitis, precancerous livers and HCC. Conversely, although phosphorylated pRb was hardly detectable in normal liver, substantial amounts of phosphorylated pRb were observed in chronic hepatitis and precancerous livers. Furthermore, its amounts were approximately 2-fold larger in HCC than in chronic hepatitis and precancerous livers. These results indicate that the cell cycle is almost completely stopped in normal liver, because no detectable phosphorylated pRb was observed in normal liver, resulting in the quiescent state of the liver. Hepatocytes in chronic hepatitis and precancerous livers are considered to be regenerating, because considerable amounts of phosphorylated pRb was observed. Furthermore, the cell cycle is turning more rapidly in HCC than in chronic hepatitis and precancerous livers, because the levels of phosphorylated pRb were the highest in HCC.

In conclusion, cyclin D1 is considered to be involved in the regeneration of hepatocytes in LEC rats, while Cdk4 may play an important role in the development of HCC in LEC rats.

Acknowledgements

This study was supported in part by a Grant-in-Aid for Scientific Research (B-14370185) from the Japanese Ministry of Education, Culture, Sports, Science and Technology.

References

1. Sasaki M, Yoshida MC, Kagami K, Takeichi N, Kobayashi H, Dempo K and Mori M: Spontaneous hepatitis in an inbread strain of Long-Evans rats. Rat News Letter 14: 4-6, 1985.
2. Yoshida MC, Masuda R, Sasaki M, Takeichi N, Kobayashi H, Dempo K and Mori M: New mutation causing hereditary hepatitis in the laboratory rat. J Hered 78: 361-365, 1987.
3. Sawaki M, Enomoto K, Takahashi H, Nakajima Y and Mori M: Phenotype of preneoplastic and neoplastic liver lesions during spontaneous liver carcinogenesis of LEC rats. Carcinogenesis 11: 1857-1861, 1990.
4. Thorgeirsson SS: The LEC rat- an animal model for human hepatitis and hepatocellular carcinoma. Jpn J Cancer Res 83: inside front cover, 1992.
5. Jong-Hon K, Togashi Y, Kasai H, Hosokawa M and Takeichi N: Prevention of spontaneous hepatocellular carcinoma in Long-Evans cinnamon rats with hereditary hepatitis by the administration of D-penicillamine. Hepatology 18: 614-620, 1993.
6. Li Y, Togashi Y, Sato S, Emoto T, Kang JH, Takeichi N, Kobayashi H, Kojima Y, Une Y and Uchino J: Spontaneous hepatic copper accumulation in Long-Evans Cinnamon rats with hereditary hepatitis. A model of Wilson's disease. J Clin Invest 87: 1858-1861, 1991.
7. Serrano M, Hannon GJ and Beach D: A new regulatory motif in cell-cycle control causing specific inhibition of cyclin D/CDK4. Nature 366: 704-707, 1993.
8. Sherr CJ: G1 phase progression: cycling on cue. Cell 79: 551-555, 1994.
9. Sherr CJ: Mammalian G1 cyclins. Cell 73: 1059-1065, 1993.
10. Matsushime H, Quelle DE, Shurtleff SA, Shibuya M, Sherr CJ and Kato J: D-type cyclin-dependent kinase activity in mammalian cells. Mol Cell Biol 14: 2066-2076, 1994.
11. Masaki T, Shiratori Y, Rengifo W, Igarashi K, Matsumoto K, Nishioka M, Hatanaka Y and Omata M: Hepatocellular carcinoma cell cycle: study of Long-Evans cinnamon rats. Hepatology 32: 711-720, 2000.
12. Laemmli UK: Cleavage of structural proteins during the assembly of the head of bacteriophage T4. Nature 227: 680-685, 1970.
13. Hanahan D and Weinberg RA: The hallmarks of cancer. Cell 100: 57-70, 2000.
14. Kang Y, Ozbun LL, Angdisen J, Moody TW, Prentice M, Diwan BA and Jakowlew SB: Altered expression of G1/S regulatory genes occurs early and frequently in lung carcinogenesis in transforming growth factor-ß1 heterozygous mice. Carcinogenesis 23: 1217-1227, 2002.
15. Hunter T and Pines J: Cyclins and cancer. Cell 66: 1071-1074, 1991.
16. Marx J: How cells cycle toward cancer. Science 263: 319-321, 1994.
17. Azechi H, Nishida N, Fukuda Y, Nishimura T, Minata M, Katsuma H, Kuno M, Ito T, Komeda T, Kita R, Takahashi R and Nakao K: Disruption of the p16/cyclin D1/retinoblastoma protein pathway in the majority of human hepatocellular carcinomas. Oncology 60: 346-354, 2001.
18. Jung YJ, Lee KH, Choi DW, Han CJ, Jeong SH, Kim KC, Oh JW, Park TK and Kim CM: Reciprocal expressions of cyclin E and cyclin D1 in hepatocellular carcinoma. Cancer Lett 168: 57-63, 2001.
19. Tetsu O and McCormick F: ß-Catenin regulates expression of cyclin D1 in colon carcinoma cells. Nature 398: 422-426, 1999.
20. Morin PJ: ß-catenin signaling and cancer. Bioessays 21: 1021-1030, 1999.
21. Ito Y, Sasaki Y, Horimoto M, Wada S, Tanaka Y, Kasahara A, Ueki T, Hirano T, Yamamoto H, Fujimoto J, Okamoto E, Hayashi N and Hori M: Activation of mitogen-activated protein kinases/extracellular signal-regulated kinases in human hepatocellular carcinoma. Hepatology 27: 951-958, 1998.
22. Masaki T, Shiratori Y, Rengifo W, Igarasi K, Yamagata M, Kurokohchi K, Uchida N, Miyauchi Y, Yoshiji H, Watanabe S, Omata M and Kuriyama S: Cyclins and cyclin-dependent kinases: comparative study of hepatocellular carcinoma versus cirrhosis. Hepatology 37: 534-543, 2003.
23. Zhang YJ, Jiang W, Chen CJ, Lee CS, Kahn SM, Santella RM and Weinstein IB: Amplification and overexpression of cyclin D1 in human hepatocellular carcinoma. Biochem Biophys Res Commun 196: 1010-1016, 1993.
24. Ito Y, Matsuura N, Sakon M, Miyoshi E, Noda K, Takeda T, Umeshita K, Nagano H, Nakamori D, Dono K, Tsujimoto M, Nakahara M, Nakao K, Taniguchi N and Monden M: Expression and prognostic roles of the G1-S modulators in hepatocellular carcinoma: p27 independently predicts the recurrence. Hepatology 30: 90-99, 1999.
25. Nishida N, Fukuda Y, Ishizaki K and Nakao K: Alteration of cell cycle-related genes in hepatocarcinogenesis. Histol Histopathol 12: 1019-1025, 1997.
26. Nishida N, Fukuda Y, Komeda T, Kita R, Sando T, Furukawa M, Amenomori M, Shibagaki I, Nakao K, Ikenaga M and Ishizaki K: Amplification and overexpression of the cyclin D1 gene in aggressive human hepatocellular carcinoma. Cancer Res 54: 3107-3110, 1994.
27. Deane NG, Parker MA, Aramandla R, Diehl L, Lee WJ, Washington MK, Nanney LB, Shyr Y and Beauchamp RD: Hepatocellular carcinoma results from chronic cyclin D1 overexpression in transgenic mice. Cancer Res 61: 5389-5395, 2001.
28. Yamagata M, Masaki T, Okudaira T, Imai Y, Shiina S, Shiratori Y and Omata M: Small hyperechoic nodules in chronic liver diseases include hepatocellular carcinomas with low cyclin D1 and Ki-67. Hepatology 29: 1722-1729, 1999.
29. Nakagawa H, Wang TC, Zukerberg L, Odze R, Togawa K, May GH, Wilson J and Rustgi AK: The targeting of the cyclin D1 oncogene by an Epstein-Barr virus promoter in transgenic mice causes dysplasia in the tongue, esophagus and forestomach. Oncogene 14: 1185-1190, 1997.
30. Nelsen CJ, Rickheim DG, Tucker MM, McKenzie TJ, Hansen LK, Pestell RG and Albrecht JH: Amino acids regulate hepatocyte proliferation through modulation of cyclin D1 expression. J Biol Chem 278: 25853-25858, 2003.
31. Schwabe RF, Bradham CA, Uehara T, Hatano E, Bennett BL, Schoonhoven R and Brenner DA: c-Jun-N-terminal kinase drives cyclin D1 expression and proliferation during liver regeneration. Hepatology 37: 824-832, 2003.
32. Jaumot M, Estanyol JM, Serratosa J, Agell N and Bachs O: Activation of cdk4 and cdk2 during rat liver regeneration is associated with intranuclear rearrangements of cyclin-cdk complexes. Hepatology 29: 385-395, 1999.
33. Kato A, Ota S, Bamba H, Wong RM, Ohmura E, Imai Y and Matsuzaki F: Regulation of cyclin D-dependent kinase activity in rat liver regeneration. Biochem Biophys Res Commun 245: 70-74, 1998.
34. Pibiri M, Ledda-Columbano GM, Cossu C, Simbula G, Menegazzi M, Shinozuka H and Columbano A: Cyclin D1 is an early target in hepatocyte proliferation induced by thyroid hormone (T3). FASEB J 15: 1006-1013, 2001.
35. Wang X, Hung NJ and Costa RH: Earlier expression of the transcription factor HFH-11B diminishes induction of $p21^{CIP1/WAF1}$ levels and accelerates mouse hepatocyte entry into S-phase following carbon tetrachloride liver injury. Hepatology 33: 1404-1414, 2001.
36. Albrecht JH, Hoffman JS, Kren BT and Steer CJ: Cyclin and cyclin-dependent kinase 1 mRNA expression in models of regenerating liver and human liver diseases. Am J Physiol 265: G857-G864, 1993.
37. Sherr CJ: Cancer cell cycles. Science 274: 1672-1677, 1996.

Proliferative capability of hepatocytes and expression of G1-related cell cycle molecules in the development of liver cirrhosis in rats

FUMI FUNAKOSHI[1], TSUTOMU MASAKI[1], YUKO KITA[1], MISUZU HITOMI[1], KAZUTAKA KUROKOHCHI[1], NAOHITO UCHIDA[1], SEISHIRO WATANABE[1], HITOSHI YOSHIJI[2] and SHIGEKI KURIYAMA[1]

[1]Third Department of Internal Medicine, Kagawa University School of Medicine, 1750-1 Ikenobe, Miki-cho, Kita-gun, Kagawa 761-0793; [2]Third Department of Internal Medicine, Nara Medical University, 840 Shijo-cho, Kashihara, Nara 634-8522, Japan

Received January 9, 2004; Accepted February 20, 2004

Abstract. Liver cirrhosis is the end stage of various chronic liver diseases and its prognosis is very poor. One of the most important causes of liver cirrhosis appears to be impaired proliferative capability of hepatocytes caused by continuous hepatic damage. Cell cycle-related molecules have been shown to play essential roles in cell proliferation. Specifically, G1-related cell cycle molecules are important, because they are requisite for the entry into the cell cycle from the quiescent state. However, the role of these cell cycle molecules during the development of liver cirrhosis remains to be examined. In the present study, liver cirrhosis was produced in rats by intraperitoneally administering dimethylnitrosamine (DMN). Proliferative capability of hepatocytes estimated immunohistochemically by proliferating cell nuclear antigen staining was markedly increased at an early stage of cirrhosis development. However, it was gradually decreased thereafter and suppressed substantially at the time of cirrhosis manifestation. Cyclin D1 expression estimated by a real-time reverse transcription-polymerase chain reaction (RT-PCR) method was also increased markedly at an early stage of cirrhosis development but decreased substantially thereafter. mRNA levels of catalytic subunits of cyclin D1, cyclin-dependent kinase 4 (Cdk4) and Cdk6, did not show significant changes during the development of liver cirrhosis. Among G1-specific Cdk inhibitors, expression of $p15^{INK4b}$ and $p16^{INK4a}$ estimated by an RT-PCR method was increased according to the progression of cirrhosis and reached a peak at the time of cirrhosis manifestation. Conversely, $p18^{INK4c}$ expression did not change significantly during the development of liver cirrhosis. These results suggest that cyclin D1 plays an essential role in hepatocyte proliferation in response to hepatic damage. However, with the decrease of cyclin D1 expression and increase of $p15^{INK4b}$ and $p16^{INK4a}$ expression, proliferative capability of hepatocytes is severely impaired and extracellular matrix components are deposited to retrieve space lost by the destruction of hepatic parenchyma, resulting in establishment of liver cirrhosis.

Correspondence to: Dr Shigeki Kuriyama, Third Department of Internal Medicine, Kagawa University School of Medicine, 1750-1 Ikenobe, Miki-cho, Kita-gun, Kagawa 761-0793, Japan
E-mail: skuriyam@kms.ac.jp

Key words: liver cirrhosis, proliferation, hepatocyte, cyclin D1, cyclin-dependent kinase, cyclin-dependent kinase inhibitor

Introduction

Because liver cirrhosis is the irreversible end stage of a variety of chronic liver injuries, such as viral hepatitis, alcoholic liver diseases, autoimmune hepatitis, metabolic disorders and parasitic diseases, the prognosis is very poor. The overall 5-year survival rate of patients with cirrhosis is comparable to that of patients with cancer of various forms. For instance, the 3-year survival of cirrhosis was 16% and the 5-year survival only 8% in a group of 308 patients after establishment of the diagnosis (1). Liver cirrhosis is a pathologically defined entity which is associated with a spectrum of characteristic clinical manifestations. The cardinal pathologic features reflect irreversible chronic injury of the hepatic parenchyma and include extensive fibrosis in association with the formation of regenerative nodules. These features result from hepatocyte necrosis, collapse of the supporting reticulin network with subsequent connective tissue deposition, distortion of the vascular bed, and nodular regeneration of remaining liver parenchyma. Among them, one of the most important causes of cirrhosis appears to be impaired proliferative capability of hepatocytes caused by continuous hepatic damage. Therefore, it is an important issue to examine the mechanism of impaired proliferative capability of hepatocytes.

Cell cycle-related molecules play essential roles in cell proliferation. Specifically, G1-related cell cycle molecules are important, because they are requisite for the entry into the cell cycle from the quiescent state (2-4). Cyclin-dependent kinases (Cdks) control the passage through the restriction point and entry into S phase. Cdks are sequentially regulated by cyclins A, D and E. Among the cyclins, D-type cyclin is the primary regulator and absolutely required for cellular progression through G1 phase of the cell cycle. Specific

cyclin/Cdk complexes are activated at different intervals during the cell cycle. Cyclin D1/Cdk4 and cyclin D1/Cdk6 are activated in mid-G1 phase. The activation of cyclin D1/Cdk4 and cyclin D1/Cdk6 complexes is responsible for the phosphorylation of retinoblastoma protein, the ultimate substrate in the pathway leading to transition from G1 to S phase. Other important G1-related cell cycle molecules include specific polypeptide inhibitors of Cdk4 and Cdk6, known as the INK family, consisting of $p15^{INK4b}$, $p16^{INK4a}$, $p18^{INK4c}$ and $p19^{INK4d}$, which can directly block cyclin D1-dependent kinase activity and cause G1 phase arrest. Thus, G1-related cell cycle molecules play essential roles in the entry into the cell cycle, resulting in cell proliferation.

Because G1-related cell cycle molecules play pivotal roles in regulation of cell cycle events. There are a number of reports showing the role of G1-related cell cycle molecules in a variety of carcinogenesis including hepatocarcinogenesis (5-11). Furthermore, there are also a number of reports demonstrating the role of G1-related cell cycle molecules in regeneration of hepatocytes (12-15). However, the role of G1-related cell cycle molecules in the process of liver cirrhosis remains to be examined. Therefore, in the present study, to examine the involvement of G1-related cell cycle molecules in the development of liver cirrhosis, we first assessed the proliferative capability of hepatocytes, and then examined mRNA expression of various G1-related cell cycle molecules, such as cyclin D1, Cdk4, Cdk6, $p15^{INK4b}$, $p16^{INK4a}$ and $p18^{INK4c}$ during the development of liver cirrhosis. Finally, we investigated whether or not altered mRNA expression levels of G1-related cell cycle molecules during the development of liver cirrhosis were correlated with the corresponding protein expression levels.

Materials and methods

Animals and chemical treatment. Six-week-old male Sprague-Dawley rats were purchased from Japan SLC (Hamamatsu, Japan). Animals were kept under a specific pathogen-free condition at 24±2°C and in a 12-h day/night light cycle with food and water available *ad libitum* throughout the experimental period. Animal experiments were performed with the approved protocols and in accordance with the institutional recommendations for the proper care and use of laboratory animals.

Chemicals were purchased from Sigma Chemical Co. (St. Louis, MO, USA) or Wako Pure Chemical Co. (Osaka, Japan), unless otherwise mentioned. To develop cirrhosis in rat liver, 1% dimethylnitrosamine (DMN) dissolved in phosphate-buffered saline (PBS) was given intraperitoneally at 1 ml per kg body weight for 3 consecutive days per week. Two, 4 and 6 weeks after the initiation of DMN treatment, livers were isolated and perfused, as described previously (16). Briefly, rats were anesthetized with ether and the abdomen was opened. The portal vein was cannulated and approximately 5 ml of a blood sample was collected from each animal. The liver was then cleared of blood with perfusion of 50 ml of PBS from the portal vein and removed for analysis of mRNA and protein expression. Untreated 8-week-old rats were also sacrificed as normal controls. Sera were obtained from the whole blood samples by centrifugation to examine biochemical parameters of DMN-treated and untreated animals. Each group consisted of 5 animals.

Histological and immunohistochemical analysis. For histological analysis, approximately half the volume of the left-lateral hepatic lobe from each animal was fixed in 10% neutral-buffered formalin, embedded in paraffin and sliced into 4 μm-thick sections. For routine histological analysis, sections were stained with hematoxylin-eosin for detecting liver injury and with Azan-Mallory dyes for detecting collagen fibers.

Liver sections were also immunohistochemically stained by the ABC method, as described previously (17). Briefly, the sections were placed in 10 mM citrate buffer (pH 6.0) and processed at 95°C for 10 min in a microwave oven. The sections were then deparaffinized with xylene, rehydrated through a graded series of alcohol solutions, and mixed with a solution containing 0.5% hydrogen peroxide to block endogenous peroxidase activity. After washing with PBS, the sections were processed for immunohistochemical staining by the ABC method. The sections were incubated overnight at room temperature with mouse monoclonal antibody anti-proliferating cell nuclear antigen (anti-PCNA) (Clone PC10: Dako; Glostrup, Denmark), with mouse monoclonal antibody anti-cyclin D1 (A-12: Santa Cruz Biotechnology; Santa Cruz, CA, USA) or with rabbit polyclonal antibody anti-p15 (K-18: Santa Cruz). All antibodies were diluted at 1:200 before use. For signal amplification, the Renaissance tyramide signal amplification kit (MEN™ Life Science Products; Boston, MA, USA) was used, as described previously (18). Immunoreactive products were visualized by using 3,3'-diaminobenzidine tetrahydrochoride (Wako), and the sections were counterstained with Mayer's hematoxylin. Nuclear labeling index for PCNA-positive cells (positive nuclei/total counted nuclei) was determined, counting at least 1000 hepatocytes in randomly selected fields of each section.

RNA extraction and reverse transcription (RT). Total RNA was extracted from approximately 30 mg of liver tissues, using the RNeasy Protect Mini Kit (Qiagen; Hilden, Germany) according to the manufacturer's instructions. Complementary DNA (cDNA) was synthesized in a 30 μl reaction volume. A sample of total RNA (2 μg) was incubated at 65°C for 10 min, and then cooled for 2 min on ice. A sample was transferred to the tube of the Ready-To-Go You-Prime First-Strand Beads (Amersham Biosciences; Piscataway, NJ, USA) and incubated for 1 min at room temperature with the oligo-dT primers (Invitrogen; Carlsbad, CA, USA). The reaction was then incubated at 37°C for 60 min. The obtained cDNA was used for quantitative real-time polymerase chain reaction (PCR).

Quantitative real-time PCR. Quantitative PCR was performed by the real-time PCR system, LightCycler (Roche Diagnostics; Mannheim, Germany), using the SYBR Green I double strand DNA binding dye (Roche Diagnostics). The amplification of a target with the primers listed in Table I was carried out in a total volume of 20 μl containing 0.3 μM of each primer, 3 mM $MgCl_2$, 2 μl of the master mixture (LightCycler FastStrand DNA Master SYBR Green I) and 1 μl of template cDNA. The reaction mixture was preheated at 95°C for 10 min, followed by 40 cycles at 95°C for 10 sec, 62°C for 10 sec and

Table I. Primers used for real-time RT-PCR.

Gene		Primers
GAPDH	For:	5'-TGAACGGGAAGCTCACTGG-3'
	Rev:	5'-TCCACCACCCTGTTGCTGTA-3'
Cyclin D1	For:	5'-GGGAAGTTTTGTTCTCTTTG-3'
	Rev:	5'-TAGTTGATTACTGGGGTACA-3'
Cdk4	For:	5'-TGTATCTTCGCAGAGATGTT-3'
	Rev:	5'-GATTAAAGGTCAGCATTTCC-3'
Cdk6	For:	5'-GACCTTTGAGCACCCCAACG-3'
	Rev:	5'-TCCAGACCTCGGAGAAGCTGA-3'
$p15^{INK4b}$	For:	5'-TCACCAGACCTGTGCATG-3'
	Rev:	5'-AGGCTGAGGACCTGCAAT-3'
$p16^{INK4a}$	For:	5'-AGGGCTTCCTAGACACTCTG-3'
	Rev:	5'-CCAGCGGAGGAGAGTAGATA-3'
$p18^{INK4c}$	For:	5'-GGAGATTGCCAGGAGACTT-3'
	Rev:	5'-CAGGCTGTGTGCTTCATTAG-3'

For: forward; Rev: reverse.

72°C for 7 sec. Fluorescence data were collected after each extension step. Melting curve analysis was performed by heating the PCR product at 95°C, then cooling to 65°C and finally raising to 95°C with a 0.1°C/sec temperature transition rate while continuously monitoring the fluorescence. Fluorescence was analyzed by using the LightCycler Software Version 3.5 (Roche Diagnostics). The crossing point for each reaction was determined and manual baseline adjustment. To quantify and prove the integrity of isolated RNA, real-time RT-PCR analysis for glyceraldehyde-3-phosphate dehydrogenase (GAPDH) was also carried out. Each run consisted of GAPDH as an internal standard and a negative control without samples.

Statistical analysis. All values are expressed as means ± SD. The significance of differences between observations was determined by Scheffe's multiple comparison method. All analyses were performed using the computer-assisted Stat View program (SAS Institute; Gary, NC, USA). A p-value of <0.05 was considered to indicate a significant difference between groups.

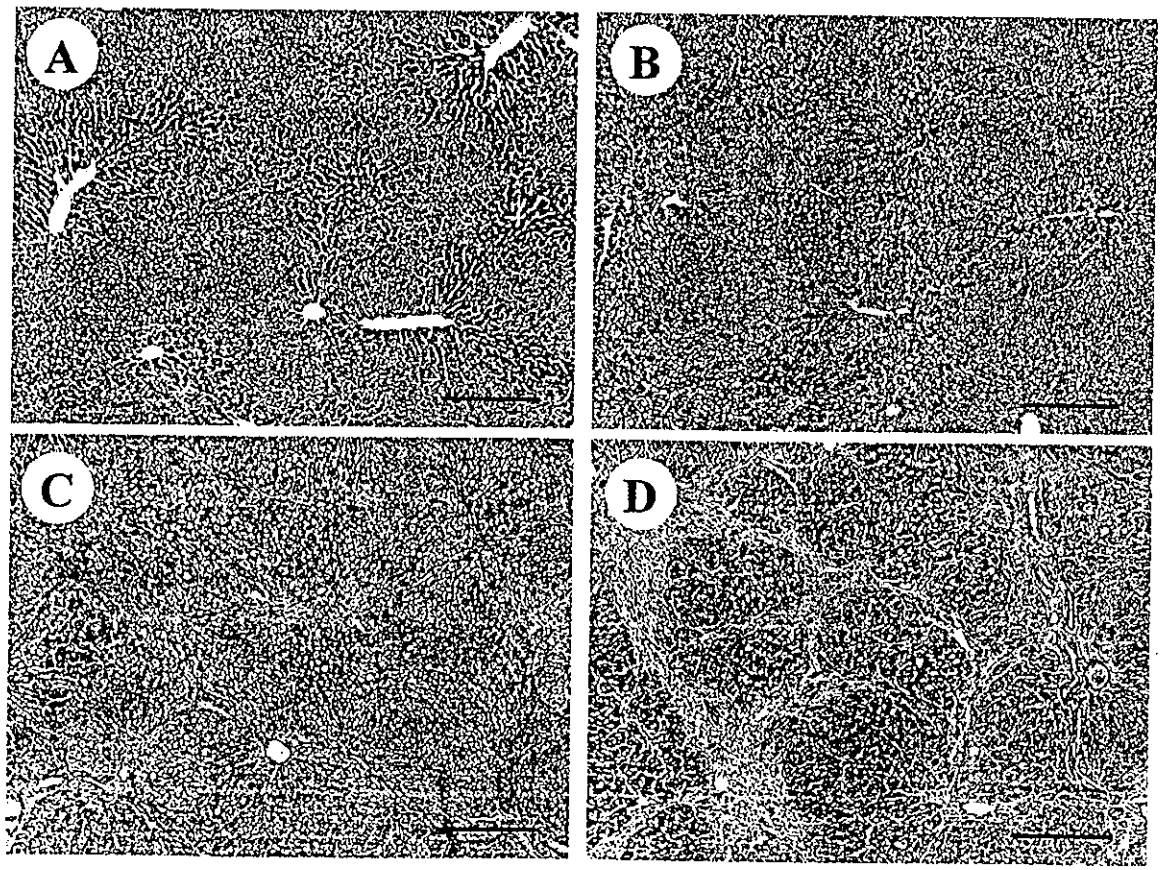

Figure 1. Azan-Mallory staining of liver sections of rats treated with DMN. To develop liver cirrhosis in rats, 1% DMN dissolved in PBS was given intraperitoneally at 1 ml per kg body weight for 3 consecutive days per week. Two, 4 and 6 weeks after the initiation of DMN treatment, livers were removed, sliced into 4-µm-thick sections and stained with Azan-Mallory dyes. There were almost no fibers in the liver of untreated normal controls (A). Fine collagen fibers were observed only at periportal regions, known as Rappaport's zone 1, in the liver of rats treated with DMN for 2 weeks (B). Azan staining of the liver of rats treated with DMN for 4 weeks demonstrated that the fibrotic septa were relatively thin and predominantly restricted to zone 1 (C). Azan staining of sections from the liver after 6-week DMN treatment revealed that cirrhosis was completely manifested by increase and thickening of the fibrotic septa, traversing the lobular parenchyma by porto-venous or porto-portal bridging, thus promoting the formation of pseudolobuli (D). Representative pictures are shown. Bars, 300 µm.

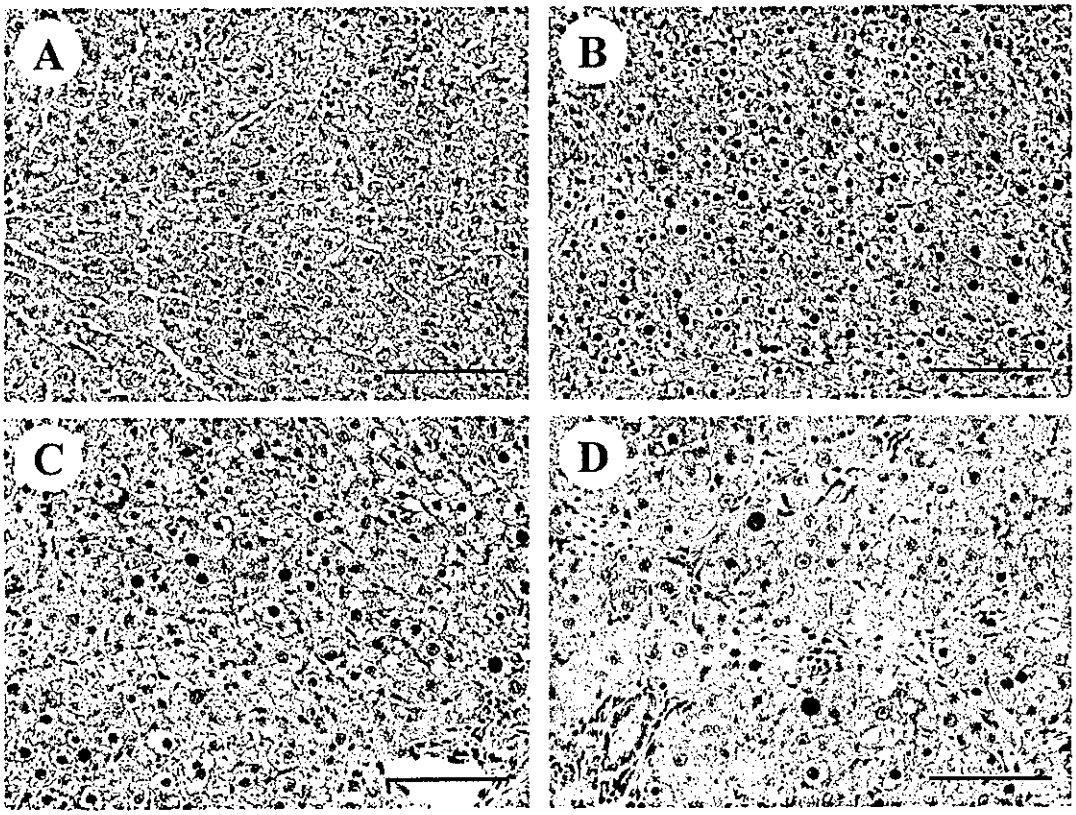

Figure 2. Immunohistochemical staining for PCNA of liver sections of rats treated with DMN. To examine the proliferating capability of hepatocytes during the development of liver cirrhosis, liver sections were stained immunohistochemically with anti-PCNA antibodies and nuclei positive for PCNA staining were examined. There were a few hepatocytes positive for PCNA staining in the liver of untreated normal controls (A). In contrast, there were a considerable number of positive hepatocytes in the liver of rats treated with DMN for 2 weeks (B). Although hepatocytes positive for PCNA staining were decreased in the liver of rats treated with DMN for 4 weeks, there were still a number of positive cells (C). Hepatocytes positive for the staining were decreased markedly in the liver of animals treated with DMN for 6 weeks (D). Representative pictures are shown. Bars, 100 μm.

Results

Histopathological findings of the liver during the development of DMN-induced liver cirrhosis in rats. Intraperitoneal administration of DMN to rats is known to cause liver cirrhosis, characterized by hepatocellular necrosis, increased connective tissue and formation of regenerative nodules. Histological analysis by hematoxylin-eosin staining of liver sections of untreated normal controls revealed that there was no infiltration of inflammatory cells. Conversely, histological analysis of liver sections of rats treated with DMN revealed infiltration of inflammatory cells including macrophages and neutrophils, and destruction of hepatic parenchyma. Hepatic damage became more severe according to the periods of DMN treatment (data not shown).

To evaluate the amount of collagen fibers in the liver, liver sections collected from DMN-treated and untreated animals were stained with Azan-Mallory dyes. There were almost no fibers in the liver of untreated normal controls (Fig. 1A). In contrast, fine collagen fibers were observed only at periportal regions, known as Rappaport's zone 1, in the liver of rats treated with DMN for 2 weeks (Fig. 1B). Azan staining of liver sections of rats treated with DMN for 4 weeks demonstrated that the fibrotic septa were relatively thin and predominantly restricted to zone 1 (Fig. 1C). Azan staining of sections from the liver after 6-week DMN treatment revealed that cirrhosis was completely manifested by increase and thickening of the fibrotic septa, traversing the lobular parenchyma by porto-venous or porto-portal bridging, thus promoting the formation of pseudolobuli (Fig. 1D).

Serum liver-related biochemical parameters of rats treated with DMN. To examine the changes of serum liver-related biochemical parameters during the development of liver cirrhosis, blood samples were collected from the portal vein when animals were sacrificed. Serum levels of albumin were decreased gradually according to the periods of DMN treatment, and the values of untreated, 2-, 4- and 6-week-treated ones were 4.3±0.2, 4.2±0.1, 3.7±0.5 and 2.6±0.4 g/dl, respectively. Serum albumin levels of animals treated with DMN for 6 weeks were significantly lower than those of both untreated, and 2- and 4-week-treated ones. Conversely, serum levels of asparate aminotransferase (AST) were increased according to the periods of DMN treatment, and the values of untreated, 2-, 4- and 6-week-treated ones were 67±5, 85±14, 117±49 and 283±56 IU/l, respectively. Serum levels of AST were significantly higher in rats treated with DMN for 6 weeks than in both untreated, and 2- and 4-week-treated ones. Serum levels of alanine aminotransferase (ALT) were also increased with time, and the values of untreated, 2-, 4-

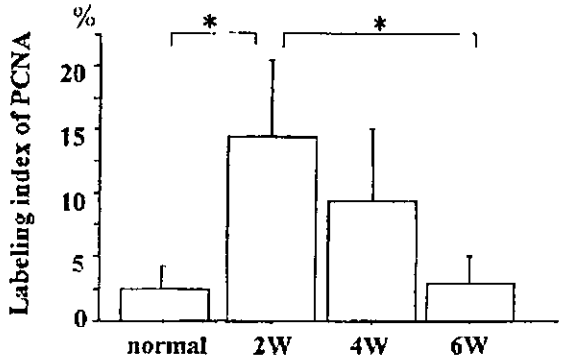

Figure 3. Quantitative estimation of hepatocytes positive for PCNA staining. The number of PCNA staining-positive nuclei of hepatocytes was significantly larger in rats treated with DMN for 2 weeks than in both untreated and 6-week-treated ones. Although the number of positive cells was larger in animals treated with DMN for 4 weeks, the values were not significantly different from those of untreated or 6-week-treated ones. There were no significant differences between untreated and 6-week-treated animals. Each bar represents the mean ± SD of 5 animals. *0.01<p<0.05.

and 6-week-treated ones were 29±7, 32±13, 71±34 and 92±43 IU/l, respectively. However, the differences were not statistically significant among the groups.

Immunohistochemical staining for PCNA. To examine the proliferating capability of hepatocytes during the development of liver cirrhosis, liver sections were stained immunohistochemically with PCNA and nuclei of hepatocytes positive for PCNA staining were counted. There were a few hepatocytes positive for PCNA staining in the liver of untreated normal controls (Fig. 2A). In marked contrast, there were a large number of positive hepatocytes in the liver of rats treated with DMN for 2 weeks (Fig. 2B). Although hepatocytes positive for PCNA staining were decreased in the liver of animals treated with DMN for 4 weeks, there were a number of positive ones (Fig. 2C). Notably, hepatocytes positive for PCNA staining were decreased markedly in the liver of animals treated with DMN for 6 weeks (Fig. 2D).

We then quantitatively evaluated the number of hepatocytes positive for PCNA staining. As shown in Fig. 3, the number of PCNA staining-positive hepatocytes was significantly larger in rats treated with DMN for 2 weeks than in both untreated and 6-week-treated ones. Although the number of positive cells was larger in animals treated with DMN for 4 weeks, the values were not significantly different compared with untreated or 6-week-treated ones. There were no significant differences between untreated and 6-week-treated animals.

Expression of cyclin D1, Cdk4 and Cdk6 during the development of liver cirrhosis. To examine expression levels of cyclin D1, Cdk4 and Cdk6 during the development of liver cirrhosis, total RNA was extracted from the liver of rats treated with DMN and mRNA levels were quantitatively evaluated by a real-time RT-PCR method. mRNA levels of cyclin D1 were increased markedly in the liver of rats treated with DMN for 2 weeks compared with untreated controls. mRNA levels of cyclin D1 were decreased slightly in the liver of rats treated with DMN for 4 weeks, and then decreased

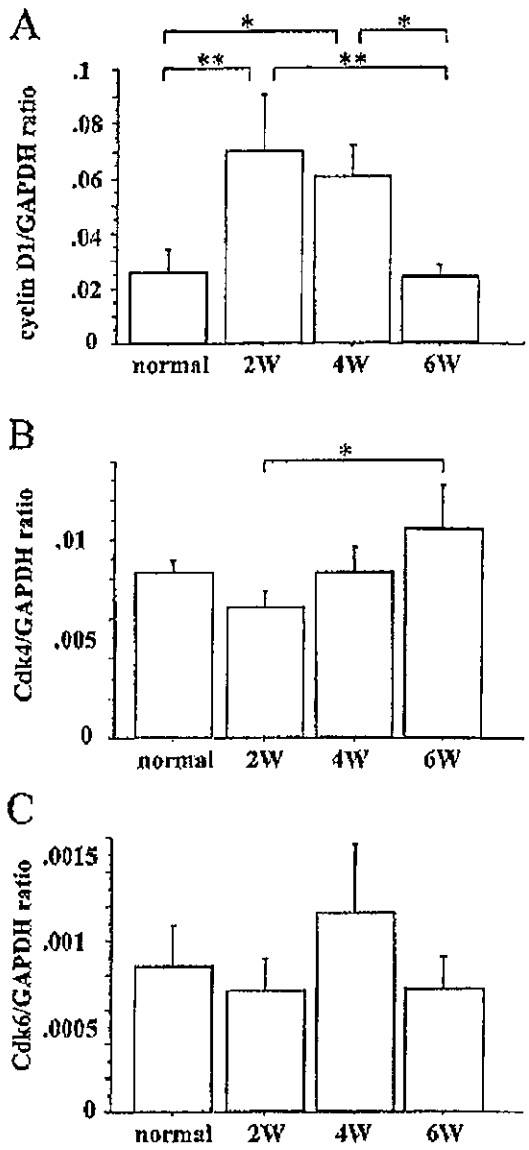

Figure 4. mRNA expression of cyclin D1, Cdk4 and Cdk6 during the development of liver cirrhosis. To quantitatively estimate mRNA expression of cyclin D1 (A), Cdk4 (B) and Cdk6 (C) during the development of liver cirrhosis, a real-time RT-PCR method was employed. The value of each amplified message was standardized by the amount of GAPDH quantified from the same sample. mRNA levels of cyclin D1 were increased markedly in the liver of rats treated with DMN for 2 weeks compared with untreated normal controls. mRNA levels of cyclin D1 were then decreased slightly in the liver of rats treated with DMN for 4 weeks, and decreased markedly in the liver of 6-week-treated ones. Statistically, mRNA levels of cyclin D1 were significantly higher in the liver of 2- and 4-week-treated animals than in untreated and 6-week-treated ones. mRNA levels of Cdk4 were elevated mildly in the liver of rats treated with DMN for 6 weeks, and the values were significantly higher than those of animals treated with DMN for 2 weeks. However, the values were not significantly different from those of untreated normal controls. mRNA levels of Cdk6 were not significantly different among the groups. Each bar represents the mean ± SD of 5 animals. *0.01<p<0.05, **0.001<p<0.01.

markedly in the liver of 6-week-treated ones. Statistically, mRNA levels of cyclin D1 were significantly higher in the liver of 2- and 4-week-treated animals than in both untreated and 6-week-treated ones (Fig. 4A).

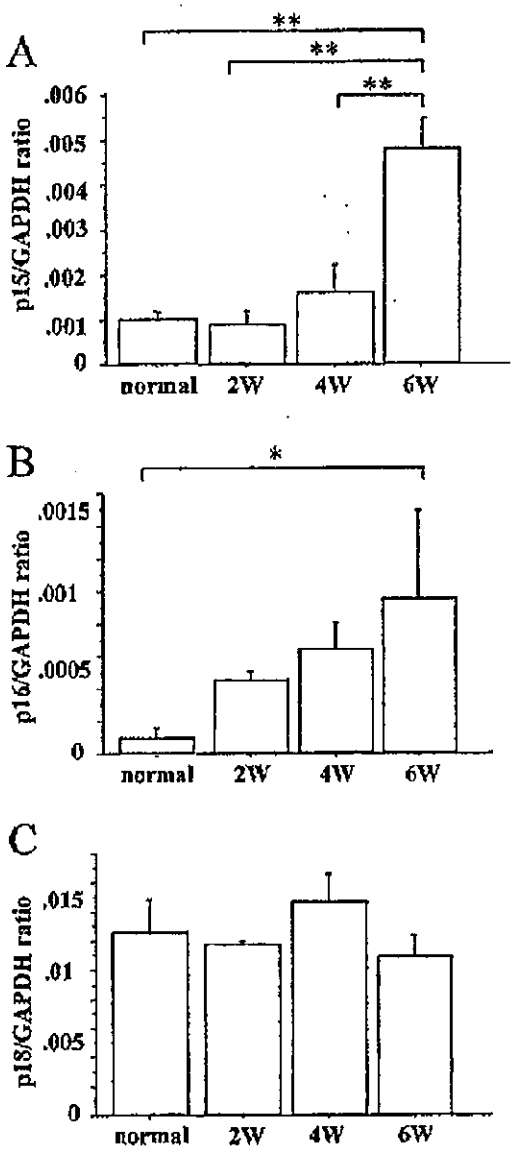

Figure 5. mRNA expression of $p15^{INK4b}$, $p16^{INK4a}$ and $p18^{INK4c}$ during the development of liver cirrhosis. To examine expression levels of the INK family during the development of liver cirrhosis, mRNA levels of $p15^{INK4b}$ (A), $p16^{INK4a}$ (B) and $p18^{INK4c}$ (C) were quantitatively evaluated by a real-time RT-PCR method. mRNA levels of $p15^{INK4b}$ were increased markedly in the liver of rats treated with DMN for 6 weeks and the values were significantly higher than those of untreated, 2- and 4-week-treated ones. mRNA levels of $p16^{INK4a}$ were also shown to increase markedly in the liver of rats treated with DMN for 6 weeks and the values were significantly higher than those of untreated normal controls. In contrast, mRNA levels of $p18^{INK4c}$ did not show any significant changes during DMN treatment. Each bar represents the mean ± SD of 5 animals. $^{*}0.001<p<0.01$, $^{**}p<0.001$.

We then examined mRNA levels of the catalytic subunits of cyclin D1, namely Cdk4 and Cdk6. mRNA levels of Cdk4 were elevated mildly in the liver of rats treated with DMN for 6 weeks, and the values were significantly higher compared with animals treated with DMN for 2 weeks. However, the values were not significantly different from those of untreated normal controls (Fig. 4B). mRNA levels of Cdk6 in the liver did not show any significant changes during the development of liver cirrhosis (Fig. 4C).

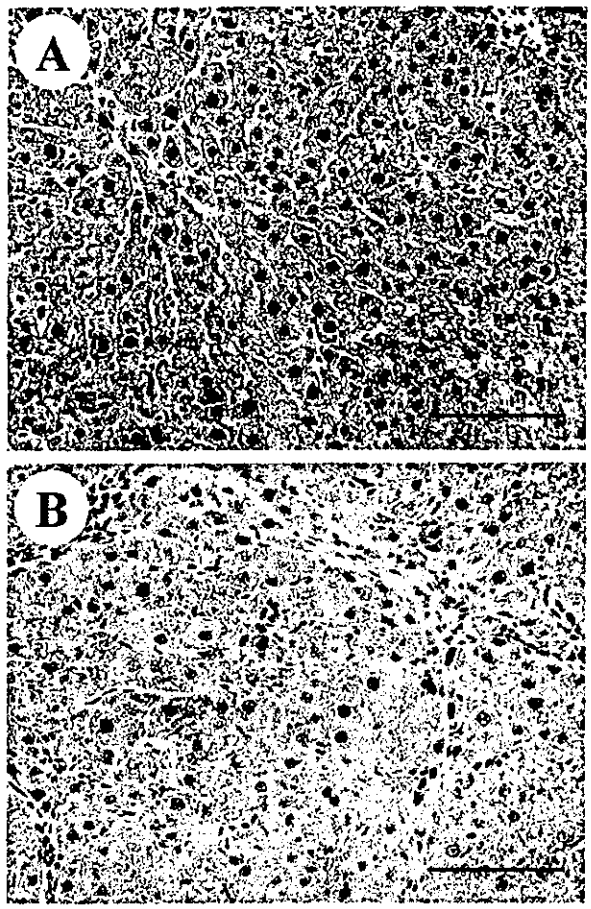

Figure 6. Immunohistochemical staining for cyclin D1 of liver sections of rats treated with DMN. To compare protein and mRNA expression during the development of liver cirrhosis, liver sections obtained from rats treated with DMN were stained immunohistochemically for cyclin D1 staining. Consistent with the results of mRNA expression of cyclin D1, there were almost no hepatocytes positive for cyclin D1 staining. In contrast, a considerable number of nuclei of hepatocytes in the liver of rats treated with DMN for 2 weeks were stained positively (A). Hepatocytes positive for cyclin D1 staining were decreased thereafter, and there were only a few positive ones in the liver of rats treated with DMN for 6 weeks (B). Representative pictures are shown. Bars, 100 μm.

Expression of $p15^{INK4b}$, $p16^{INK4a}$ and $p18^{INK4c}$ during the development of liver cirrhosis. To examine expression levels of the INK family during the development of liver cirrhosis, mRNA levels of $p15^{INK4b}$, $p16^{INK4a}$ and $p18^{INK4c}$ were evaluated quantitatively by real-time RT-PCR. mRNA levels of $p15^{INK4b}$ were increased markedly in the liver of rats treated with DMN for 6 weeks and the values were significantly higher compared with those of untreated, 2- and 4-week-treated ones (Fig. 5A). mRNA levels of $p16^{INK4a}$ were also increased markedly in the liver of animals treated with DMN for 6 weeks and the values were significantly higher compared with those of untreated controls (Fig. 5B). Conversely, mRNA levels of $p18^{INK4c}$ did not show any significant changes during the development of liver cirrhosis in rats treated with DMN for various time periods (Fig. 5C).

Immunohistochemical staining for cyclin D1 and $p15^{INK4b}$ of the liver of rats treated with DMN. To compare expression

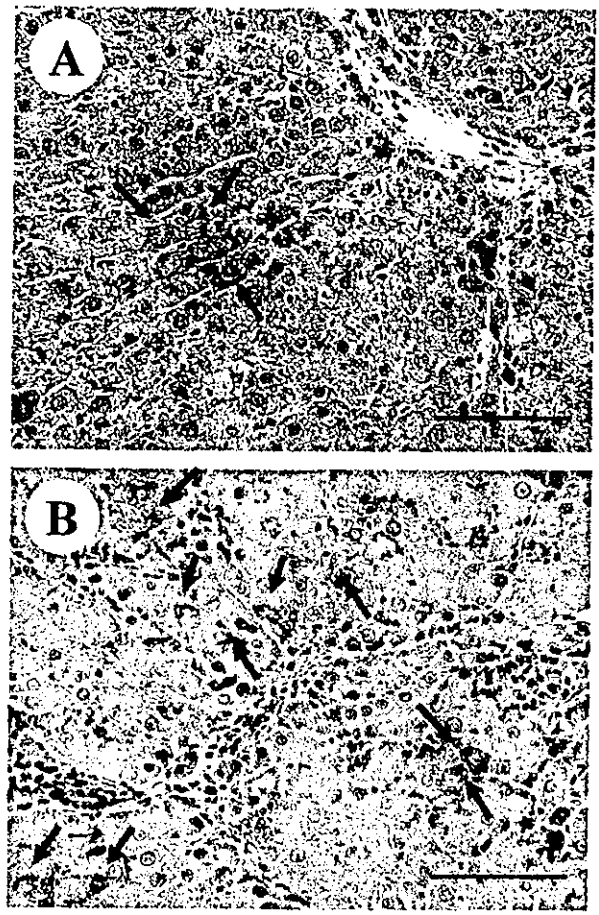

Figure 7. Immunohistochemical staining for $p15^{INK4b}$ of liver sections of rats treated with DMN. There were almost no hepatocytes positive for $p15^{INK4b}$ staining not only in the liver of untreated normal controls but also in that of rats treated with DMN for 2 weeks. Only a small number of hepatocytes in the liver of rats treated with DMN for 4 weeks were stained positively with $p15^{INK4b}$ staining in the cytoplasm (A). In contrast, there were a number of hepatocytes with the cytoplasm positive for $p15^{INK4b}$ staining in the liver of rats treated with DMN for 6 weeks (B). Arrows indicate hepatocytes with the cytoplasm positive for $p15^{INK4b}$ staining. Representative pictures are shown. Bars, 100 µm.

levels of mRNA and protein during the development of liver cirrhosis, liver sections obtained from rats treated with DMN were stained immunohistochemically for cyclin D1 and $p15^{INK4b}$. Consistent with the results of mRNA expression, there were few hepatocytes positive for cyclin D1 staining in the liver of untreated normal controls (data not shown). In contrast, a number of positive hepatocytes were detected in liver sections obtained from rats treated with DMN for 2 weeks (Fig. 6A). Hepatocytes positive for cyclin D1 staining were decreased thereafter, and there were only a few positive ones in the liver of rats treated with DMN for 6 weeks (Fig. 6B).

With regard to immunohistochemical staining for $p15^{INK4b}$, there were few hepatocytes positive for $p15^{INK4b}$ staining not only in the liver of untreated normal controls but also in the liver of rats treated with DMN for 2 weeks (data not shown). Only a small number of hepatocytes positive for $p15^{INK4b}$ staining were observed in liver sections obtained from rats treated with DMN for 4 weeks (Fig. 7A). In contrast, a number of positive hepatocytes were detected in the liver of rats treated with DMN for 6 weeks (Fig. 7B).

Discussion

Although the liver is highly capable of regeneration, continuous liver damage caused by viral infection, alcohol, autoimmune-related diseases, metabolic disorders or hepatic toxins lead to cirrhosis. Liver cirrhosis is characterized by a marked accumulation of extracellular matrix components and tissue remodeling. Theses phenomena are induced to retrieve space lost by destruction of hepatic parenchyma. Therefore, one of the most important causes of liver cirrhosis appears to be impaired proliferative capability of hepatocytes. Repeated intraperitoneal administration of DMN has been shown to cause hepatocyte destruction and production of extracellular matrix components mainly composed of collagen fibers, resulting in manifestation of cirrhosis (19-22). In the present study, we first examined the proliferative capability of hepatocytes during the development of liver cirrhosis, using an animal liver cirrhosis model induced by DMN treatment. PCNA is a stable cell cycle-related nuclear protein, 36 kDa in molecular weight, which is increasingly expressed in late G1 and throughout S phase of the cell cycle. Its rate of synthesis is correlated with the proliferative rate of cells (23-27). Several studies comparing PCNA immunohistochemistry with established proliferation markers indicate that immunostaining of PCNA can be used to define and map proliferating cells in animal and human tissues and that this method represents a reliable marker for the determination of proliferative activity (28-31). Therefore, we employed an immunohistochemical PCNA-staining method to assess the proliferative capability of hepatocytes during the development of liver cirrhosis. At an early stage of the continuous hepatic damage caused by DMN, a number of hepatocytes with nuclei positive for PCNA staining were observed. However, PCNA-positive hepatocytes were then decreased gradually and there were a very small number of PCNA-positive ones at the establishment of liver cirrhosis. These results indicate that although hepatocytes can proliferate in response to hepatic damages for certain time periods, the proliferative capability of hepatocytes is exhausted during continuously lasting hepatic damage. This exhaustion of the proliferative capability of hepatocytes is considered to be a main cause of the development of liver cirrhosis. Accordingly, the next important issue to be examined is why hepatocytes lose the proliferative capability during the development of liver cirrhosis.

Cell cycle-related molecules play essential roles in cell proliferation. Specifically, G1-related cell cycle molecules are important, because they are requisite for the entry into the cell cycle from the quiescent state. Therefore, it is considered that disruption of the regulation of G1-related cell cycle molecules is contributed to the development of liver cirrhosis. However, little is known about disproportion of these molecules during the development of liver cirrhosis. Cell cycle-related molecules are mainly divided into 3 groups, namely cyclins, Cdks and Cdk inhibitors. Among cyclins, cyclin D1 serves as a critical regulator of the cell cycle (32). The cyclin D1 gene

has been identified as a target gene in the Wnt signaling pathway as well as the Ras-activated mitogen-activated protein kinase signaling pathway. It has been shown that cyclin D1 expression is markedly increased in rodent livers after partial hepatectomy (12-15). It has also been shown that cyclin D1 induction is one of the earlier events in hepatocyte proliferation induced by thyroid hormone (33), suggesting that cyclin D1 may be a common target responsible for the mitogenic activity of ligands of nuclear receptors. Furthermore, it has been shown by differential hybridization of cDNA arrays and RNase protection studies that early stimulated expression of cyclin D1 was induced in the murine liver treated with a hepatotoxic compound CCl_4 (34). Furthermore, Albrecht *et al* (35) have demonstrated the increased cyclin D1 expression in human liver tissues from various acute and chronic liver diseases, and stated that cyclin D1 may eventually provide a clinically relevant molecular marker of regenerative activity in human liver diseases. We have also demonstrated that cyclin D1 might play a major role in hepatocyte proliferation but not in hepatocarcinogenesis, because its expression was increased in the course of chronic hepatic inflammation and decreased in hepatocellular carcinoma. Taken collectively, these results indicate that the induction of cyclin D1 plays an essential role in hepatocyte proliferation. In the present study, we demonstrated that mRNA levels of cyclin D1 were increased markedly at an early stage of chronic hepatic damage. mRNA levels of cyclin D1 were then decreased during the course of chronic hepatic damage and significantly reduced at the time of manifestation of liver cirrhosis. There were no significant differences in cyclin D1 mRNA level between undamaged normal and cirrhotic livers. Similar results were confirmed by the subsequent immunohistochemical staining for cyclin D1, indicating that both mRNA and protein levels of cyclin D1 were increased for a certain time period in response to hepatic damage but then decreased during further continuing hepatic damage.

Cyclin D1 binds and activates the catalytic subunits, Cdk4 and Cdk6. Cyclin D1/Cdk4 and cyclin D1/Cdk6 complexes phosphorylate retinoblastoma protein, resulting in transition from G1 to S phase (1-4). Cyclin D1 forms complexes with Cdk4 and also with Cdk6. Therefore, the cyclin D1-related kinase activities can be expressed as the sum of cyclin D1/Cdk4 and cyclin D1/Cdk6 kinase activities. Levels of Cdk4 and Cdk6 do not always correlate with each other. For instance, it has been shown that in the regenerating liver of mice after partial hepatectomy, cyclin D1 formed complexes with Cdk4, which were markedly activated in the regenerating liver, but not with Cdk6 (36). We have also shown that mRNA and protein expression of Cdk4 was higher in the chronic hepatitis liver than in the normal liver (11). Therefore, enhanced kinase activity of cyclin D1/Cdk4, but not cyclin D1/Cdk6, was considered to be responsible for hepatocyte proliferation. In the present study, it was shown that levels of Cdk4 mRNA were increased slowly during the development of liver cirrhosis and values were significantly higher in rats treated with DMN for 6 weeks than in those for 2 weeks. However, there were no significant differences between untreated normal controls and 6-week-treated rats. With regard to Cdk6 mRNA levels, no significant differences were observed among untreated, 2-, 4- and 6-week-treated animals. Taken collectively, the results with regard to cyclin D1, Cdk4 and Cdk6 demonstrated in the present study suggest that cyclin D1 but not Cdk4 nor Cdk6 plays a critical role in hepatocyte regeneration in response to hepatic damage.

For the regulation of cell cycle, cyclin-dependent kinase inhibitors (CKIs) also play essential roles. CKIs are currently classified into 2 groups (37). The first group, known as the CIP-KIP family, consists of $p21^{Waf1}$, $p27^{Kip1}$ and $p57^{Kip2}$. Because these inhibitors require preformed cyclin/Cdk complexes for binding and are able to inhibit all kinds of cyclin/Cdk complexes (38-42), molecules of the CIP-KIP family are not G1 phase-specific. The second group of CKIs, known as the INK family, consists of $p15^{INK4b}$, $p16^{INK4a}$, $p18^{INK4c}$ and $p19^{INK4d}$. Unlike the CIP-KIP family, these inhibitors are active only on Cdk4- or Cdk6-containing complexes. In addition, binding of the INK family proteins to Cdk4 or to Cdk6 is independent of cyclin D (43-47). Because members of this family are known to bind and inhibit Cdk4 and Cdk6 without affecting other Cdks (3), they are G1 phase-specific. Therefore, to examine the role of G1-related cell cycle molecules, we evaluated the expression of $p15^{INK4b}$, $p16^{INK4a}$ and $p18^{INK4c}$ mRNA. It was shown in the present study that mRNA levels of $p15^{INK4b}$ and $p16^{INK4a}$ were increased during the development of liver cirrhosis and elevated markedly in the cirrhotic liver of rats treated with DMN for 6 weeks. In marked contrast, mRNA levels of $p18^{INK4c}$ were not changed significantly during the development of liver cirrhosis. These results indicate that markedly impaired proliferative capability of hepatocytes at a late stage of cirrhosis development may be caused by increased $p15^{INK4b}$ and $p16^{INK4a}$ expression but not by unchanged $p18^{INK4c}$ expression.

In conclusion, during the course of cirrhosis development, hepatocytes reveal high proliferative capability in response to hepatic damage, which appears to be induced by augmented cyclin D1 expression. However, according to the time periods of continuous hepatic damage, hepatocytes gradually lose their proliferative capability, which appears to be caused not only by decreased cyclin D1 expression but also by increased $p15^{INK4b}$ and $p16^{INK4a}$ expression. Therefore, the strategy to maintain high levels of cyclin D1 expression or to suppress $p15^{INK4b}$ and $p16^{INK4a}$ expression may be effective to inhibit the development of liver cirrhosis.

Acknowledgements

This work was supported in part by a Grant-in-Aid for Scientific Research (B-14370185) from the Japanese Ministry of Education, Culture, Sports, Science and Technology.

References

1. Creutzfeldt W and Beck K: Cirrhosis of the liver. On the aetiology, pathogenesis, results of treatment and period of survival in an unselected series of 560 patients. Ger Med Mon 11: 259-265, 1966.
2. Sherr CJ: Mammalian G_1 cyclins. Cell 73: 1059-1065, 1993.
3. Sherr CJ: Cancer cell cycles. Science 274: 1672-1677, 1996.
4. Sandal T: Molecular aspects of the mammalian cell cycle and cancer. Oncologist 7: 73-81, 2002.
5. Nishida N, Fukuda Y, Komeda T, Kita R, Sando T, Furukawa M, Amenomori M, Shibagaki I, Nakao K, Ikenaga M and Ishizaki K: Amplification and overexpression of the cyclin D1 gene in aggressive human hepatocellular carcinoma. Cancer Res 54: 3107-3110, 1994.

6. Masaki T, Shiratori Y, Rengifo W, Igarashi K, Matsumoto K, Nishioka M, Hatanaka Y and Omata M: Hepatocellular carcinoma cell cycle: study of Long-Evans Cinnamon rats. Hepatology 32: 711-720, 2000.
7. Deane NG, Parker MA, Aramandla R, Diehl L, Lee W-J, Washington MK, Nanney LB, Shyr Y and Beauchamp RD: Hepatocellular carcinoma results from chronic cyclin D1 overexpression in transgenic mice. Cancer Res 61: 5389-5395, 2001.
8. Pascale RM, Simile MM, De Miglio MR, Muroni MR, Calvisi DF, Asara G, Casabona D, Frau M, Seddaiu MA and Feo F: Cell cycle deregulation in liver lesions of rats with and without genetic predisposition to hepatocarcinogenesis. Hepatology 35: 1341-1350, 2002.
9. Masaki T, Shiratori Y, Rengifo W, Igarashi K, Yamagata M, Kurokohchi K, Uchida N, Miyauchi Y, Yoshiji H, Watanabe S, Omata M and Kuriyama S: Cyclins and cyclin-dependent kinases: comparative study of hepatocellular carcinoma versus cirrhosis. Hepatology 37: 534-543, 2003.
10. Azechi H, Nishida N, Fukuda Y, Nishimura T, Minata M, Katsuma H, Kuno M, Ito T, Komeda T, Kita R, Takahashi R and Nakao K: Disruption of the p16/cyclin D1/retinoblastoma protein pathway in the majority of human hepatocellular carcinomas. Oncology 60: 346-354, 2001.
11. Kita Y, Masaki T, Funakoshi F, Yoshida S, Tanaka M, Kurokohchi K, Uchida N, Watanabe S, Matsumoto K and Kuriyama S: Expression of G1 phase-related cell cycle molecules in naturally developing hepatocellular carcinoma of Long-Evans Cinnamon rats. Int J Oncol 24: 1205-1211, 2004.
12. Nelsen CJ, Rickheim DG, Tucker MM, McKenzie TJ, Hansen LK, Pestell RG and Albrecht JH: Amino acids regulate hepatocyte proliferation through modulation of cyclin D1 expression. J Biol Chem 278: 25853-25858, 2003.
13. Schwabe RF, Bradham CA, Uehara T, Hatano E, Bennett BL, Schoonhoven R and Brenner DA: c-Jun-N-terminal kinase drives cyclin D1 expression and proliferation during liver regeneration. Hepatology 37: 824-832, 2003.
14. Jaumot M, Estanyol JM, Serratosa J, Agell N and Bachs O: Activation of cdk4 and cdk2 during rat liver regeneration is associated with intranuclear rearrangements of cyclin-cdk complexes. Hepatology 29: 385-395, 1999.
15. Kato A, Ota S, Bamba H, Wong RM, Ohmura E, Imai Y and Matsuzaki F: Regulation of cyclin D-dependent kinase activity in rat liver regeneration. Biochem Biophys Res Commun 245: 70-74, 1998.
16. Kuriyama S, Tsujimoto T, Nakatani Y, Tsujinoue H, Yoshiji H, Mitoro A, Yamazaki M, Okuda H, Toyokawa Y, Nagao S, Nishiwaki I and Fukui H: Sonographic estimation of liver tumor development induced by oral administration of thioacetamide in rat. In Vivo 13: 129-134, 1999.
17. Masaki T, Tokuda M, Fujimura T, Ohnishi M, Tai Y, Miyamoto K, Itano T, Matsui H, Watanabe S, Sogawa K, Yamada T, Konishi R, Nishioka M and Hatase O: Involvement of annexin I and annexin II in hepatocyte proliferation: can annexins I and II be markers for proliferative hepatocytes? Hepatology 20: 425-435, 1994.
18. Yamagata M, Masaki T, Okudaira T, Imai Y, Shiina S, Shiratori Y and Omata M: Small hyperechoic nodules in chronic liver diseases include hepatocellular carcinomas with low cyclin D1 and Ki-67 expression. Hepatology 29: 1722-1729, 1999.
19. Yasuda H, Imai E, Shiota A, Fujise N, Morinaga T and Higashio K: Antifibrogenic effect of a deletion variant of hepatocyte growth factor on liver fibrosis in rats. Hepatology 24: 636-642, 1996.
20. Baroni GS, D'Ambrosio L, Curto P, Casini A, Mancini R, Jezequel AM and Benedetti A: Interferon gamma decreases hepatic stellate cell activation and extracellular matrix deposition in rat liver fibrosis. Hepatology 23: 1189-1199, 1996.
21. Ueno T, Sujaku K, Tamaki S, Ogata R, Kin M, Nakamura T, Sakamoto M, Torimura T, Mitsuyama K, Sakisaka S, Sata M and Tanikawa K: OK-432 treatment increases matrix metalloproteinase-9 production and improves dimethyl-nitrosamine-induced liver cirrhosis in rats. Int J Mol Med 3: 497-503, 1999.
22. Yasuda M, Shimizu I, Shiba M and Ito S: Suppressive effects of estradiol on dimethylnitrosamine-induced fibrosis of the liver in rats. Hepatology 29: 719-727, 1999.
23. Bravo R, Fey SJ, Bellatin J, Larsen PM, Arevalo J and Celis JE: Identification of a nuclear and a cytoplasmic polypeptide whose relative proportions are sensitive to changes in the rate of cell proliferation. Exp Cell Res 136: 311-319, 1981.
24. Mathews MB, Bernstein RM, Franza BR Jr and Garrels JI: Identity of the proliferating cell nuclear antigen and cyclin. Nature 309: 374-376, 1984.
25. Bravo R, Frank R, Blundell PA and MacDonald-Bravo H: Cyclin/PCNA is the auxiliary protein of DNA polymerase δ. Nature 326: 515-517, 1987.
26. Prelich G, Tan CK, Kostura M, Mathews MB, So AG, Downey KM and Stillman B: Functional identity of proliferating cell nuclear antigen and a DNA polymerase-delta auxiliary protein. Nature 326: 517-520, 1987.
27. Morris GF and Mathews MB: Regulation of proliferating cell nuclear antigen during the cell cycle. J Biol Chem 264: 13856-13864, 1989.
28. Garcia RL, Coltrera MD and Gown AM: Analysis of proliferative grade using anti-PCNA/cyclin monoclonal anti-bodies in fixed, embedded tissues. Am J Pathol 134: 733-739, 1989.
29. Wolf HK and Michalopoulos GK: Hepatocyte regeneration in acute fulminant and nonfulminant hepatitis: a study of proliferating cell nuclear antigen expression. Hepatology 15: 707-713, 1992.
30. Weisgerber UM, Boeing H, Nemitz R, Raedsch R and Waldherr R: Proliferation cell nuclear antigen (clone 19A2) correlates with 5-bromo-2-deoxyuridine labelling in human colonic epithelium. Gut 34: 1587-1592, 1993.
31. Rudi J, Waldherr R, Raedsch R and Kommerell B: Hepatocyte proliferation in primary biliary cirrhosis as assessed by proliferating cell nuclear antigen and Ki-67 antigen labelling. J Hepatol 22: 43-49, 1995.
32. Hanahan D and Weinberg RA: The hallmarks of cancer. Cell 100: 57-70, 2000.
33. Pibiri M, Ledda-Columbano GM, Cossu C, Simbula G, Menegazzi M, Shinozuka H and Columbano A: Cyclin D1 is an early target in hepatocyte proliferation induced by thyroid hormone (T3). FASEB J 15: 1006-1013, 2001.
34. Wang X, Hung NJ and Costa RH: Earlier expression of the transcription factor HFH-11B diminishes induction of $p21^{CIP1/WAF1}$ levels and accelerates mouse hepatocyte entry into S-phase following carbon tetrachloride liver injury. Hepatology 33: 1404-1414, 2001.
35. Albrecht JH, Hoffman JS, Kren BT and Steer CJ: Cyclin and cyclin-dependent kinase 1 mRNA expression in models of regenerating liver and human liver diseases. Am J Physiol 265: G857-G864, 1993.
36. Rickheim DG, Nelsen CJ, Fassett JT, Timchenko NA, Hansen LK and Albrecht JH: Differential regulation of cyclins D1 and D3 in hepatocyte proliferation. Hepatology 36: 30-38, 2002.
37. Sherr CJ and Roberts JM: Inhibitors of mammalian G1 cyclin-dependent kinases. Genes Dev 9: 1149-1163, 1995.
38. Harper JW, Adami GR, Wei N, Keyomarsi K and Elledge SJ: The p21 cdk-interacting protein Cip1 is a potent inhibitor of G1 cyclin-dependent kinases. Cell 75: 805-816, 1993.
39. Lee MH, Reynisdottir I and Massague J: Cloning of $p57^{KIP2}$, a cyclin-dependent kinase inhibitor with unique domain structure and tissue distribution. Genes Dev 9: 639-649, 1995.
40. Polyak K, Kato J, Solomon MJ, Sherr CJ, Massague J, Roberts JM and Koff A: $p27^{Kip1}$, a cyclin-cdk inhibitor, links transforming growth factor-ß and contact inhibition to cell cycle arrest. Genes Dev 8: 9-22, 1994.
41. Polyak K, Lee M, Erdjument-Bromage H, Koff A, Roberts JM, Tempst P and Massague J: Cloning of $p27^{Kip1}$, a cyclin-dependent kinase inhibitor and a potential mediator of extracellular anti-mitogenic signals. Cell 78: 59-66, 1994.
42. Xiong Y, Hannon GJ, Zhang H, Casso D, Kobayashi R and Beach D: p21 is a universal inhibitor of cyclin kinases. Nature 366: 701-704, 1993.
43. Chan FK, Zhang J, Cheng L, Shapiro DN and Winoto A: Identification of human and mouse p19, a novel CDK4 and CDK6 inhibitor with homology to $p16^{Ink4}$. Mol Cell Biol 15: 2682-2688, 1995.
44. Guan KL, Jenkins CW, Li Y, Nichols MA, Wu X, O'Keefe CL, Matera AG and Xiong Y: Growth suppression by p18, a $p16^{INK4/MTS1}$- and $p14^{INK4/MTS2}$-related Cdk6 inhibitor, correlates with wild-type pRb function. Genes Dev 8: 2939-2952, 1994.
45. Hannon GJ and Beach D: $p15^{INK4b}$ is a potential effector of TGF-ß-induced cell cycle arrest. Nature 371: 257-261, 1994.
46. Hirai H, Roussel MF, Kato JY, Ashmun RA and Sherr CJ: Novel INK4 proteins, p19 and p18, are specific inhibitors of the cyclin D-dependent kinases Cdk4 and Cdk6. Mol Cell Biol 15: 2672-2681, 1995.
47. Serrano M, Hannon GJ and Beach D: A new regulatory motif in cell-cycle control causing specific inhibition of cyclinD/Cdk4. Nature 366: 704-707, 1993.

Halting the Interaction Between Vascular Endothelial Growth Factor and Its Receptors Attenuates Liver Carcinogenesis in Mice

Hitoshi Yoshiji,[1] Shigeki Kuriyama,[2] Junichi Yoshii,[1] Yasuhide Ikenaka,[1] Ryuichi Noguchi,[1] Daniel J. Hicklin,[3] Yan Wu,[3] Koji Yanase,[1] Tadashi Namisaki,[1] Mitsuteru Kitade,[1] Masaharu Yamazaki,[1] Hirohisa Tsujinoue,[1] Tsutomu Masaki,[2] and Hiroshi Fukui[1]

It has been shown that angiogenesis plays an important role not only in tumor growth, but also in early carcinogenesis. The expression of a potent angiogenic factor, vascular endothelial growth factor (VEGF), increased during the early stage of carcinogenesis. In this study, the effects of the neutralizing monoclonal antibodies R1 mAb and R2 mAb of the VEGF receptors Flt-1 (VEGFR-1) and KDR/Flk-1 (VEGFR-2), respectively, on murine hepatocarcinogenesis induced by diethylnitrosamine (DEN) were examined. The effects of R1 mAb and R2 mAb on spontaneous lung metastasis from hepatocellular carcinoma (HCC) were also investigated. VEGF expression and neovascularization in the tumor increased stepwise during hepatocarcinogenesis. Treatment with both R1 mAb and R2 mAb markedly inhibited the development of HCC and adenoma in the liver. The inhibitory effect of R2 mAb was more potent than that of R1 mAb, and the combination treatment with both mAbs almost completely attenuated hepatocarcinogenesis. Both R1 mAb and R2 mAb treatment significantly suppressed the development of angiogenesis in HCC. The suppressive effects against angiogenesis R1 mAb and R2 mAb were similar in magnitude to their inhibitory effects against hepatocarcinogenesis. Furthermore, spontaneous lung metastasis from HCC was also significantly suppressed by R1 mAb and R2 mAb treatment. In conclusion, these results suggest that VEGF and receptor interaction plays an important role in hepatocarcinogenesis and in spontaneous lung metastasis from HCC. (HEPATOLOGY 2004;39:1517–1524.)

Tumor survival, growth, and subsequent metastasis are underpinned by the recruitment of new blood vessels.[1–3] Without angiogenesis, a tumor cannot grow even beyond a few millimeters in size. In addition to mature tumor growth, evidence indicates that induction of angiogenesis precedes the formation of malignant tumors, suggesting that angiogenesis is a rate-limiting step not only in tumor growth but also in carcinogenesis.[4,5] It has been reported that alterations in the hepatic microcirculation occur at the early stages of liver carcinogenesis, in association with liver cell change or within dysplastic nodules, before the emergence of morphologically identifiable hepatocellular carcinoma (HCC) in human samples.[6] Another clinical report showed that angiogenesis in the liver gradually increased from low-grade dysplastic nodules during hepatocarcinogenesis.[7] In an experimental study, a semisynthetic analogue of fumagilin, TNP-470, which possesses antiangiogenic activity, suppressed the progression of HCC.[8]

Angiogenesis is regulated by the net balance between proangiogenic factors and angiogenic inhibitors.[1,2] To date, many positive and negative angiogenic-modulating factors have been identified, and the vascular endothelial growth factor (VEGF), also known as vascular permeability factor, is the most intrusive factor with regard to angiogenesis.[9,10] Emerging evidence shows that VEGF plays a pivotal role in many physiological as well as pathological angiogenic processes. In contrast to other angiogenic fac-

Abbreviations: HCC, hepatocellular carcinoma; VEGF, vascular endothelial growth factor; mAb, neutralizing monoclonal antibody; EC, endothelial cells; Flt-1, Fms-like tyrosine kinase; KDR/Flk-1, kinase-insert domain-containing receptor/fetal liver kinase-1; DEN, diethylnitrosamine; IgG, immunoglobulin G; PBS, phosphate buffer saline; mRNA, messenger RNA; PCR, polymerase chain reaction.

From the [1]Third Department of Internal Medicine, Nara Medical University, Nara, Japan; [2]Third Department of Internal Medicine, Kagawa Medical University, Kagawa, Japan; and [3]Department of Immunology, ImClone Systems Incorporated, New York.

Received June 18, 2003; accepted February 13, 2004.

Address reprint requests to: H. Yoshiji, MD, PhD, Third Department of Internal Medicine, Nara Medical University, Shijo-cho 840, Kashihara, Nara 634-8522, Japan. E-mail: yoshijih@naramed-u.ac.jp; fax: 81-744-24-7122.

Published online in Wiley InterScience (www.interscience.wiley.com).
DOI 10.1002/hep.20218

tors, VEGF acts almost exclusively on endothelial cells (EC) and is also known as a survival factor for EC.[11,12] Without VEGF, apoptosis is rapidly induced in EC.[13] It has been shown that VEGF has a critical, nonredundant role in the transgenic mouse model of pancreatic β-cell carcinogenesis.[14] In HCC, several studies have shown that VEGF expression was upregulated more in the tumor lesion than in noncancerous tissues.[15–17] We have reported that overexpression of VEGF correlated with a marked increase in murine HCC tumor growth, in addition to augmentation of neovascularization, and that HCC growth was tightly regulated by VEGF expression.[18] Two tyrosine kinases, *Fms*-like tyrosine kinase (Flt-1), or VEGFR-1, and the kinase insert domain-containing receptor fetal liver kinase-1 (KDR/Flk-1), or VEGFR-2, both of which are type III tyrosine kinase receptors, have been identified as the main VEGF receptors. These two receptors serve different biological roles in many pathological events,[10,19] and VEGFR-2 plays a more important role than VEGFR-1 *in vitro* and *in vivo*.[19–22] Previously, we reported that inhibition of VEGF and VEGFR-2 interaction significantly reduced the tumor growth and angiogenesis of HCC.[23] A recent study has revealed that, in addition to VEGFR-2, VEGFR-1 also played an important role under certain conditions of pathological angiogenesis, such as tumor growth.[24–26] It has also been reported that VEGFR-1 played an important role in the experimental lung metastasis from melanoma and Lewis lung carcinoma cells.[26] However, the roles of VEGFR-1 and VEGFR-2 in hepatocarcinogenesis and lung metastasis from HCC have not been yet examined.

In the present study, we elucidated the biological role of VEGF and receptor interaction using the specific neutralizing monoclonal antibodies of VEGFR-1 and VEGFR-2 (R1 mAb and R2 mAb, respectively) in liver carcinogenesis, in conjunction with angiogenesis development. We also examined the effects of R1 mAb and R2 mAb on spontaneous lung metastasis from HCC.

Materials and Methods

Animals. Male BALB/c mice, aged 6 weeks, were purchased from Japan SLC, Inc. (Hamamatsu, Shizuoka, Japan). They were housed in stainless-steel mesh cages under controlled conditions of temperature (23 ± 3°) and relative humidity (50% ± 20%), with 10 to 15 air changes per hour and light for 12 hours per day. The animals were allowed access to food and tap water *ad libitum* throughout the acclimatization and experimental periods.

Compounds and Animal Treatment. R1 mAb and R2 mAb were provided by ImClone Systems (New York, NY) as previously described.[27,28] It has been shown that R2 mAb exerted a VEGFR-2 inhibitory effect in a dose-dependent manner, and that the maximal effect was achieved at a dose of 1,000 μg/mouse twice per week.[28,29] We therefore employed this dose in our current study.

The experimental period in all experiments was 36 weeks. The mice were divided into 5 groups (n = 18 each; G1, G2, G3, G4, and G5). The mice in G1 to G4 received an intraperitoneal injection of 75 mg/kg of diethylnitrosamine (DEN) weekly for 3 weeks, then 100 mg/kg of DEN for 3 weeks followed by phenobarbital mixed with each meal at a concentration of 0.05% from week 6 to the final sacrifice as described previously.[30, 31] R1 mAb and R2 mAb were administered intraperitoneally to the mice of G2 and G3 twice a week. In G4, both R1 mAb and R2 mAb were administered simultaneously. The animals in G1 received the same amount of a control immunoglobulin G (IgG) as described previously.[23, 32, 33] The mice that received phosphate buffer saline (PBS) instead of DEN were examined as a negative control group (G5). All mice were anesthetized, the thoracic cavity was opened, and blood samples were withdrawn via cardiac puncture. Alanine aminotransferase and total bilirubin were assessed by routine laboratory methods. All animal procedures were performed according to standard protocols and in accordance with the standard recommendations for the proper care and use of laboratory animals.

Tumor Examinations. Entire livers from randomly chosen mice in each group (n = 10) were removed, weighed, and cut into 2-mm-thick strips to examine the presence of macroscopically visible lesions. All macroscopic lesions were described, mapped, and quantitated by size as described previously.[34] The liver strips were fixed in 4% paraformaldehyde for 24 hours, embedded in paraffin, and stained with hematoxylin-eosin. The histological examination of the hepatocellular neoplasms was classified as described previously.[31,35] Two independent certified pathologists performed the histological assessment in a blind manner. The liver sections of G1 to G5 were randomly given to the investigators, who confirmed the same diagnosis with later discussion. We also examined spontaneous lung metastasis from the DEN-induced HCC. After fixation of the lung, low-power (×10) microscopic examination was performed to detect and count the metastatic lesions in the lungs.

Expression of VEGF and CD31 in the Tumor. The messenger RNA (mRNA) expressions of VEGF and CD31, which are used widely as markers of neovascularization, were evaluated by real-time polymerase chain reaction (PCR). The protein expressions of VEGF and CD31 were also examined by Western blot and immunohistochemical analysis, respectively, as described previ-

ously.[33,36] The macroscopically visible tumor lesions and the adjacent tissues were separated, and half of the tumor tissue was immediately snap-frozen for RNA and protein extraction (n = 5 in each experimental group). The other half of the tissue samples was fixed in 4% paraformaldehyde for the pathological examinations or OCT compound for the immunohistochemical examinations. We used the same size of tumor to avoid the necrotic effect of the hypoxic conditions as previously described.[33] Real-time PCR was performed with the ABI Prism 7700 Sequence Detection System (Perkin Elmer Applied Biosystems, Foster City, CA) according to the manufacturer's manual. Relative quantitation of gene expression was performed as described in the manual by using glyceraldehyde-3-phosphate dehydrogenase as an internal control. The threshold cycle and the standard curve method were used for calculating the relative amount of the target RNA as described for PE. To prevent genomic DNA contamination, all RNA samples were subjected to DNase I digestion and checked by 40 cycles of PCR to confirm the absence of amplified DNA. The CD31-positive microvessel length was assessed under ×200 magnification. In each tumor sample, 5 areas showing the highest density of staining were selected for counting. In counting, the large vessels with a thick muscular wall or with a lumen greater than 50 μm in diameter were excluded. These immunopositive vessels were evaluated with Adobe Photoshop and NIH image software as previously described.[33] The protein expression level of VEGF was determined by Western Blot analysis as previously described,[37] using an amplified alkaline phosphatase immunoblot assay kit (Bio-Rad, Hercules, CA) and antibody against VEGF (sc-507) (Santa Cruz, Santa Cruz, CA).

Immunoprecipitation. To examine whether R1 mAb and R2 mAb at a dose of 1,000 μg/mouse suppressed autophosphorylation of the receptors in the HCC lesion, immunoprecipitation was performed as previously described.[33,36] Fifteen minutes after R1 mAb and R2 mAb were intraperitoneally injected, the tumor was resected from 3 mice in each group and snap-frozen immediately. From the tumor tissues, which were pathologically diagnosed as HCC, pool lysate solutions were concentrated and used for immunoprecipitation. To conduct immunoprecipitation, the HCC lysates were immunoprecipitated with antiphosphotyrosine before conducting sodium dodecyl sulfate polyacrylamide gel electrophoresis. Anti-tyrosine (4G10) was purchased from Upstate Biotechnology (Lake Placid, NY) and anti-VEGFR-2 (C-1158), -VEGFR-1 (C-17) were obtained from Santa Cruz. Before the Western blotting, we stained each membrane with Ponceau solution (Sigma, St. Louis, MO) to confirm that the same amounts of protein were immunoprecipitated (data not shown). Blots were developed using an amplified alkaline phosphatase immunoblot assay kit (Bio-Rad).

Statistical Analysis. To assess the statistical significance of intergroup differences in the quantitative data, Bonferroni's multiple comparison test was used after one-way ANOVA. This was followed by Barlett's test to determine the homology of variance.

Table 1. Effect of R1 mAb and R2 mAb on Several Markers In DEN-Treated Liver

	Body Weight (g)	Relative Liver Weight (%)	Total Bilirubin (mg/dL)	ALT (U/L)
Control	38.2 ± 6.4	6.2 ± 0.7	0.4 ± 0.1	142.4 ± 31.8
R1 mAb	37.2 ± 6.0	5.2 ± 0.6*	0.4 ± 0.1	148.8 ± 28.3
R2 mAb	37.1 ± 5.4	4.8 ± 0.8*	0.3 ± 0.1	133.8 ± 30.8
R1 + R2 mAb	38.8 ± 5.3	4.6 ± 0.6*	0.4 ± 0.1	154.7 ± 32.8
PBS	38.8 ± 5.3	4.6 ± 0.6*	0.4 ± 0.1	144.7 ± 27.8

Abbreviations: ALT, adanine aminotransferase; PBS, phosphate buffer saline.
*$P < .01$ vs. control.

Results

General and Macroscopic Findings. All mice survived throughout the experimental period. As shown in Table 1, there were no significant differences in final body weight among the groups. On the other hand, the relative liver weight (liver weight/body weight) was significantly higher in G1 than in the other groups, possibly due to development of the liver tumors. Figure 1A shows the typical pale white macroscopic appearance of the hepatic lesions. Treatment with DEN resulted in marked development of hepatic nodules (Fig. 2). The total number of hepatic nodules was significantly suppressed by treatment with R1 mAb and R2m Ab (G2 and G3, respectively), and the combination treatment of R1 mAb and R2 mAb exerted further inhibition (G4). The inhibitory effect of R2 mAb was much more potent than that of R1 mAb ($P < .01$). In the 3 tumor-size categories, there were many large nodules in the control group. Conversely, the ratio of small nodules increased in the R1 mAb- and R2 mAb-treated groups. No hepatic nodule was found in the PBS-treated group (G5), and neither ascites nor other organ abnormalities were observed at the end of the experiment, with the exception of lung metastasis (data not shown). R1 mAb and R2 mAb treatment did not cause any alteration in the serum liver functional markers, suggesting that the inhibitory effects of R1 mAb and R2 mAb against hepatic nodule development were not secondary re-

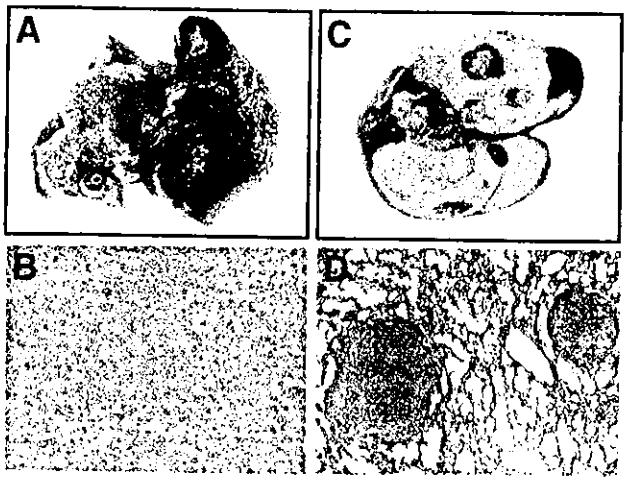

Fig. 1. Typical gross and microscopic features of HCC and lung metastasis. (A) The typical multiple hepatic nodules in the DEN-treated liver (G1) were whitish and their margins were relatively clear. (B) HCC mostly displayed a trabecular pattern with cords of more than 1 hepatocyte in thickness and partially demonstrated a pseudoglandular pattern. (C) Multiple metastatic lung nodules were observed in the DEN-treated group (G1). (D) Histological features of lung metastasis in mice from the DEN-treated group. Magnification (B) ×200 and (D) ×40.

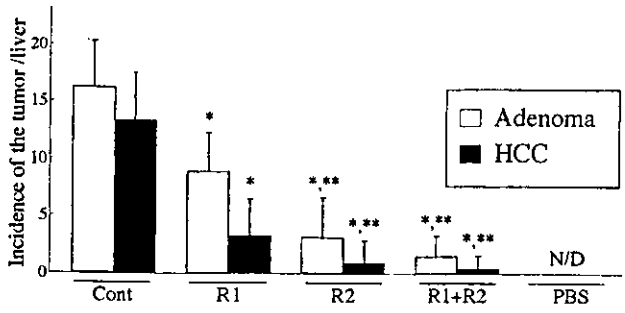

Fig. 3. Effects of R1 mAb and R2 mAb on the microscopic development of HCC and adenoma in the liver. The incidences of both adenoma and HCC in the liver were significantly inhibited by treatments with R1 mAb and R2 mAb. The combination treatment of R1 mAb and R2 mAb almost completely attenuated development of the liver neoplasm. Similar to the macroscopic findings of hepatic nodules, the inhibitory effect of R2 mAb was significantly stronger than that of R1 mAb in the development of both adenoma and HCC. Data represent mean ± SD (n = 10). Cont, control IgG-treated mice (1,000 μg/mouse [G1]); R1 and R2, R1 mAb- and R2 mAb-treated mice (1,000 μg/mouse [G2 and G3, respectively]); R1 + R2, R1 mAb and R2 mAb combination-treated group (G4); PBS, phophate buffer saline-treated group (G5); N/D: not detected. *Statistically significant difference from G1 ($P < .01$). **Statistically significant difference from G2 ($P < .05$).

sponses to the cytoprotective effect against DEN (Table 1).

Histological Examination. Histological examination of the hepatic nodules displayed hepatocellular adenoma and HCC. The adenoma consisted of foci of well-differentiated hepatocytelike cells that formed regular cords (1 cell in thickness). The adenoma compressed the surrounding nonfocal hepatocyte cytoplasm. HCC displayed a trabecular pattern with cords of more than 1 hepatocyte in thickness and partially exerted a pseudoglandular pattern (Fig. 1B). The incidences of adenoma and HCC in the liver were significantly inhibited by treatment with R1 mAb and R2 mAb (Fig. 3). The combination treatment of R1 mAb and R2 mAb almost completely attenuated the development of liver neoplasm. Similar to the macroscopic findings of the hepatic nodules, the inhibitory effect of R2 mAb was significantly stronger than that of R1 mAb against the development of both adenoma and HCC ($P < .01$). No evidence of tumor development could be found in the PBS-treated group.

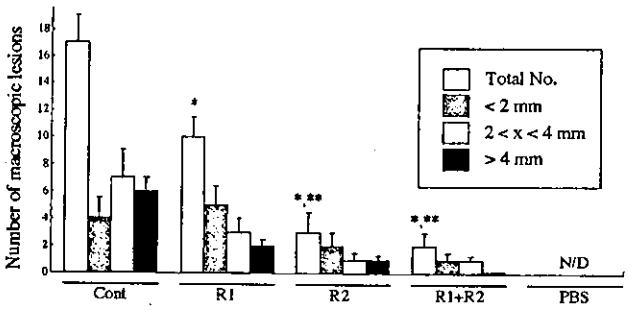

Fig. 2. Effects of R1 mAb and R2 mAb on the mean number and size of macroscopic hepatic nodules. The total number of the hepatic nodules was significantly suppressed by treatments with both R1 mAb and R2 mAb (G2 and G3, respectively), and the combination treatment of R1 mAb and R2 mAb exerted further inhibition (G4). Phophate buffer saline (PBS)-treated group (G5). The inhibitory effect of R2 mAb was much more potent than that of R1mAb ($P < .01$). In the 3 tumor-size categories, there were many large nodules in the control group. Conversely, the ratio of small nodules increased in both R1 mAb- and R2 mAb-treated groups. No hepatic nodule was found in the PBS-treated group (G5). Data represent mean ± SD (n = 10). Cont, control IgG-treated mice (1,000 μg/mouse [G1]); R1 and R2, R1 mAb- and R2 mAb-treated mice (1,000 μg/mouse [G2 and G3, respectively]); R1 + R2, R1 mAb and R2 mAb combination-treated group (G4); PBS, phophate buffer saline-treated group; N/D, not detected. *Statistically significant difference from G1 ($P < .01$). **Statistically significant difference from G2 ($P < .05$).

VEGF Expression and Neovascularization in the Tumor. First, we examined whether the VEGF and CD31 mRNA expressions were altered during liver carcinogenesis. Figure 4 demonstrates that VEGF mRNA expressions increased stepwise during hepatocarcinogenesis in addition to augmentation of neovascularization. The VEGF and CD31 mRNA expressions in the adenoma and HCC were significantly upregulated compared with the adjacent nontumor lesions ($P < .05$ and $P < .01$, respectively). We performed preliminary routine reverse transcriptase-PCR and found that, among the alternative splicing variants of the mouse VEGF genes, $VEGF_{164}$ and $VEGF_{120}$ were abundant forms in the DEN-treated liver (data not shown). Next, we examined the effects of R1

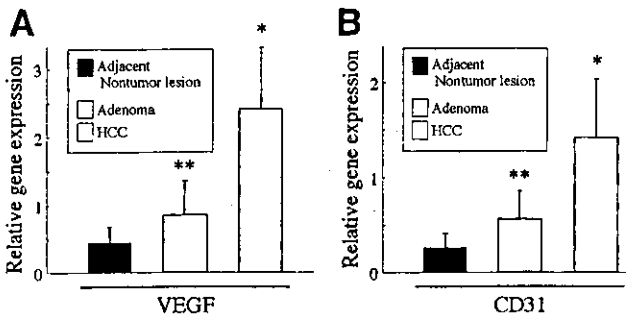

Fig. 4. VEGF and CD31 mRNA expressions in the DEN-treated liver. The mRNA expression was examined by real-time PCR as described in Materials and Methods. The mRNA expressions of VEGF and CD31 increased stepwise during hepatocarcinogenesis. (A) VEGF and (B) CD31 expressions in the adenoma and HCC were significantly upregulated compared with the adjacent nontumor lesions ($P < .05$ and $P < .01$, respectively). Data represent mean ± SD (n = 5). *Statistically significant difference from the adjacent nontumor lesions ($P < .01$). **Statistically significant difference from the adjacent nontumor lesions ($P < .05$).

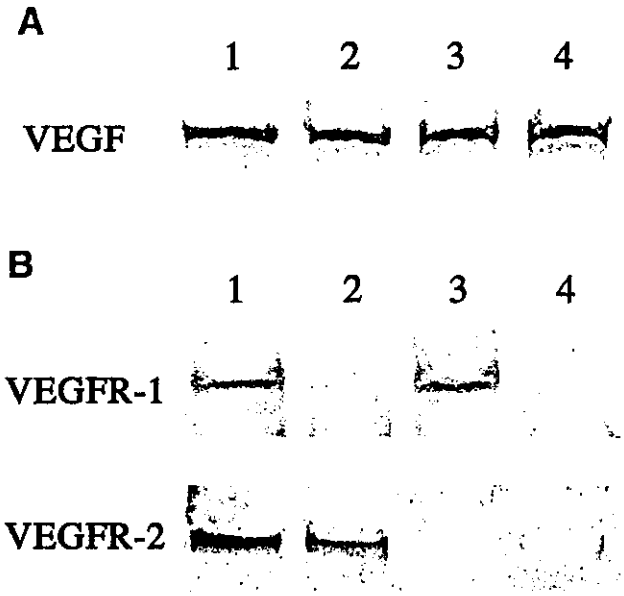

Fig. 6. Effects of R1 mAb and R2 mAb on (A) VEGF expression and (B) activation of VEGFR-1 and VEGFR-2 receptors in HCC tissue. (A) Similar to mRNA expression, neither R1 mAb treatment nor R2 mAb treatment altered the VEGF protein expression in HCC tissue. (B) R1 mAb and R2 mAb significantly inhibited tyrosine phosphorylation of the respective receptors. Neither the activation of VEGFR-1 nor that of VEGFR-2 was altered by the administration of R2 mAb and R1 mAb, respectively. **Lane 1**, IgG-treated control group (G1). **Lane 2**, R1 mAb-treated group (G2). **Lane 3**, R2 mAb-treated group (G3). **Lane 4**, R1 mAb and R2 mAb combination-treated group (G4).

mAb and R2 mAb on VEGF and CD31 expressions in HCC tissue. The VEGF mRNA and protein expressions in HCC did not change with either R1 mAb or R2 mAb treatment (Figs. 5A and 6A). Alternatively, both R1 mAb and R2 mAb significantly suppressed CD31 mRNA expressioncompared to the control group ($P < .01$). The inhibitory impact of R2 mAb was more potent than that of R1 mAb treatment ($P < .01$), and the combination treatment of both mAbs almost abolished neovascularization in HCC (Fig. 5B). We also examined the intratumoral microvessel density. Figures 7A and B (low and high magnification, respectively) show representative features of CD31-positive vessels in the tumor. The results of semiquantitation of the microvessels in the tumor were similar to those of CD31 mRNA expression in the tumor (Fig. 7C), suggesting that the ECs were a target for these mAbs and resulting in alteration of intratumoral angiogenesis. Of note was the finding that the suppression of angiogenesis by treatment with R1 mAb and R2 mAb was of similar magnitude as that of the inhibition of liver neoplasm development.

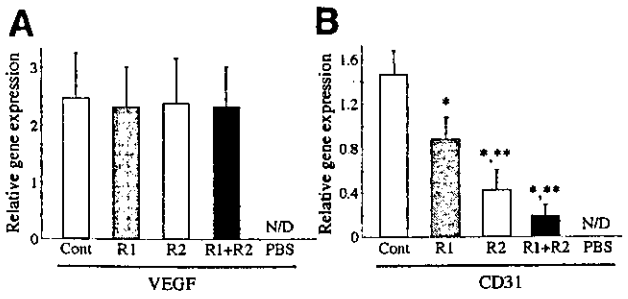

Fig. 5. Effects of R1 mAb and R2 mAb on the mRNA expressions of VEGF and CD31 in HCC. The mRNA expressions were examined by real-time PCR as described in Materials and Methods. (A)VEGF expression in HCC. Neither R1 mAb treatment nor R2 mAb treatment altered VEGF gene expression in the HCC tissue. (B) Both R1 mAb and R2 mAb significantly suppressed CD31 gene expression as compared to the control group. The inhibitory impact of R2 mAb was more potent than that of R1 mAb treatment, and the combination treatment of both mAbs almost abolished CD31 expression in the liver. Data represent mean ± SD (n = 5). Cont, control IgG-treated mice (1,000 μg/mouse [G1]); R1 and R2, R1 mAb- and R2 mAb-treated mice (1,000 μg/mouse [G2 and G3, respectively]); R1 + R2, R1 mAb and R2 mAb combination-treated group (G4); PBS, phosphate buffer saline-treated group (G5); N/D: not detected. *Statistically significant difference from G1 ($P < .01$). **Statistically significant difference from G2 ($P < .05$).

***Receptor Activation* In Situ.** It has been reported that the inhibitory effects of R1 mAb and R2 mAb on receptor activation are dose-dependent.[28,29] To examine whether or not R1 mAb and R2 mAb at the dose used in the current study (1,000 μg/mouse) actually inhibited autophosphorylation in the tumor, we analyzed tyrosine-phosphorylated VEGFR-1 and VEGFR-2 after intraperitoneal injection of R1 mAb and R2 mAb. We observed phosphorylated bands of VEGFR-1 and VEGFR-2 at about 180 kd and 230 kd respectively, as mentioned in previous reports.[13,38] R1 mAb and R2 mAb significantly inhibited tyrosine phosphorylation of the receptors in HCC, and the activation of VEGFR-1 and VEGFR-2 was